OXFORD UNIVERSITY PRESS | Cerebral Cortex

Human parahippocampal cortex supports spatial binding in visual working memory

Journal:	*Cerebral Cortex*
Manuscript ID	CerCor-2016-01170.R2
Manuscript Type:	Original Articles
Date Submitted by the Author:	14-Jul-2017
Complete List of Authors:	Dundon, Neil; Bangor University, School of Psychology; University of Freiburg, Department of Child and Adolescent Psychiatry, Psychotherapy and Psychosomatics Katshu, Mohammad; University of Nottingham Faculty of Medicine and Health Sciences, Division of Psychiatry and Applied Psychology Harry, Bronson; Western Sydney University Bankstown campus, The MARCS Institute for Brain, Behaviour and Development Roberts, Daniel; Liverpool John Moores University Faculty of Science, School of Natural Sciences and Psychology Leek, Charles; Bangor University, School of Psychology; Universite Grenoble Alpes, Laboratoire de Psychologie et NeuroCognition (LPNC) Downing, Paul; Bangor University, School of Psychology Sapir, Ayelet; Univ Wales, Bangor, School of Psychology Roberts, Craig; Betsi Cadwaladr University Health Board, North Wales Brain Injury Service d'Avossa, Giovanni; Bangor University, School of Psychology; Betsi Cadwaladr University Health Board, North Wales Brain Injury Service
Keywords:	Visual working memory, Parahippocampal cortex, Spatial Memory, Medial temporal lobe, Feature binding

Human parahippocampal cortex supports spatial binding in visual working memory

Neil Michael Dundon[1,2], Mohammad Zia Ul Haq Katshu[3], Bronson Harry[4], Daniel Roberts[5], E. Charles Leek[1,6], Paul Downing[1], Ayelet Sapir[1], Craig Roberts[7], Giovanni d'Avossa[1,7]

[1]Bangor University, School of Psychology; [2]University of Freiburg, Department of Child and Adolescent Psychiatry, Psychotherapy and Psychosomatics; [3]University of Nottingham Faculty of Medicine and Health Sciences, Division of Psychiatry and Applied Psychology; [4]Western Sydney University Bankstown campus, The MARCS Institute for Brain, Behaviour and Development; [5]Liverpool John Moores University Faculty of Science, School of Natural Sciences and Psychology; [6]Universite Grenoble Alpes, Laboratoire de Psychologie et NeuroCognition (LPNC); [7]Betsi Cadwaladr University Health Board, North Wales Brain Injury Service

Corresponding author:

Giovanni d'Avossa**,**

School of Psychology - Brigantia Building,

Bangor University,

Bangor, LL572AS,

Gwynedd, UK.

Tel: +441248388801 / Fax: +441248382599

Email: g.davossa@bangor.ac.uk

Running title: Human PHC supports spatial binding

Abstract

Studies investigating the functional organisation of the medial temporal lobe (MTL) suggest that parahippocampal cortex (PHC) generates representations of spatial and contextual information used by the hippocampus in the formation of episodic memories. However, evidence from animal studies also implicates PHC in spatial binding of visual information held in short term, working memory. Here we examined a 46-year-old man (PJ), after he had recovered from bilateral medial occipitotemporal cortex strokes resulting in ischemic lesions of PHC and hippocampal atrophy, and a group of age-matched healthy controls. When recalling the colour of one of two objects, PJ misidentified the target when cued by its location, but not shape. When recalling the position of one of three objects, he frequently misidentified the target, which was cued by its colour. Increasing the duration of the memory delay had no impact on the proportion of binding errors, but did significantly worsen recall precision in both PJ and controls. We conclude that PHC may play a crucial role in spatial binding during encoding of visual information in working memory.

Keywords: Feature binding; Medial temporal lobe; Parahippocampal cortex; Spatial Memory; Visual working memory

Introduction

The medial temporal lobe (MTL) comprises the hippocampus and parahippocampal regions, i.e., entorhinal cortex, perirhinal cortex (PRC) and parahippocampal cortex (PHC). These structures play a prominent role in episodic memory, as evidenced by the dense anterograde amnesia, which follows damage to MTL (Scoville and Milner 1957; Corkin 1984; Corkin et al. 1997). Modular accounts of MTL function have suggested that the hippocampus synthesises episodic memories by binding information about the identity and location of objects carried respectively by two different streams (Eichenbaum et al. 2007; Diana et al. 2007).

MTL structures have also been implicated in short term memory processes (Ranganath and Blumenfeld 2005; Graham et al. 2010; Yonelinas, 2013). First, animal models have pointed to specific molecular mechanisms in the mammalian MTL dedicated to the storage of short term memories, and separate from those involved in long term memory (Deacon et al. 2002; Reisel et al. 2002). Single unit recordings and lesion studies in non-human primates have further demonstrated that the hippocampus (Friedman and Goldman-Rakic 1988), entorhinal cortex (Suzuki et al. 1997), PRC (Davachi and Goldman-Rakic 2001) and PHC (Bachevalier and Nemanic 2008) contribute to the encoding and recall of information from short term memory. These animal findings complement neuropsychological studies of patients with amnesia resulting from Korsakoff's Syndrome, encephalitis and colloid cysts (Holdstock et al. 1995), and patients with surgical (Aggleton 1992; Owen et al. 1995) or ischemic (Holdstock et al. 2002) lesions to the MTL, demonstrating retention deficits for novel stimuli over delay intervals as short as two seconds (Ranganath and Blumenfeld 2005).

An increasing body of evidence further suggests that short term memory exploits the same MTL modules as episodic memory; that is, PRC codes information about an object's identity and PHC codes an object's location and its context, and these two streams are bound in the hippocampus (Pertzov et al. 2013; Watson et al. 2013; Yee et al. 2014; Libby et al. 2014). Consistent with the idea that in short term memory identity and location information are processed separately and then bound, patients with hippocampal damage can exhibit deficits recalling object-location conjunctions after 1.0s delays, even when unimpaired recalling either object identities or locations (Olson et al. 2006a; 2006b). However, other studies report that patients with damage to the hippocampus do not necessarily show deficits in recalling object-location conjunctions, suggesting that spatial binding is preserved (e.g. Jeneson et al. 2010; see Yonelinas 2013 for a review).

An alternative possibility is that spatial binding in short term memory occurs in parahippocampal regions, rather than the hippocampus proper. In support of this view, data in both rats (Burwell and Amaral 1998) and monkeys (Suzuki and Amaral 1994) indicate that PRC and PHC are reciprocally connected, suggesting that the parcellation of identity and spatial information is not absolute, and that there may already be substantial cross-talk between object and spatial/context related information in parahippocampal regions. Further, recordings in rats have demonstrated single unit responses for object-location conjunctions in the PHC homologue (Barker and Warburton 2011).

Behavioural studies in monkeys have provided crucial evidence for the role of PHC in spatial binding. Rhesus monkeys with PHC lesions are impaired in both simple location and object-location conjunction tasks (Malkova and Mishkin, 2003). This short term memory impairment was observed in a delayed match-to-sample task, where the sample contained two non-identical objects. After a six-second delay, the test array contained one of the objects in its original location (the target), and an identical item either at the location of the sample foil (object-place condition), or at a novel location not previously occupied by either sample object (location condition). Monkeys with PHC lesions were impaired identifying the target in both conditions, while monkeys with lesions in the hippocampus showed no impairment in either task (Malkova and Mishkin 2003). Hippocampectomised monkeys were likewise unimpaired in a later study, using a more difficult task with an increased number of objects and locations (Belcher et al. 2006).

A cross-species homology in the short term memory functionality of PHC is partly supported by the observation that patients with PHC lesions also exhibit a decrement in spatial recall (Ploner et al. 2000), although this impairment is only observed using delays greater (i.e. >15.0s) than those used by Malkova and Mishkin (2003). In addition, functional imaging data in healthy subjects demonstrate heightened right PHC activation during both encoding and maintenance of object-location conjunctions, relative to trials where objects or locations are memorised separately (Luck et al. 2010). However, no neuropsychological study has so far demonstrated that PHC contributes to spatial binding in human short term memory.

In the present study, we examined the nature and extent of spatial and short term memory deficits associated with focal PHC lesions, by testing a middle-aged man (PJ) with bilateral posterior circulation strokes involving the PHC, but sparing the hippocampus and PRC. Our experiments were driven by three specific research questions: 1) does damage to PHC produce binding difficulties and if so, are the binding problems specifically spatial or do they generalise to other visual dimensions; 2) do binding impairments reflect deficits in memory encoding or maintenance; and 3) is the binding impairment secondary to a loss of positional information either in memory or perception?

Both PJ and controls showed dependent decrements in the precision of spatial recall, however PJ's recall precision was significantly worse than controls at longer delays (5.0s). PJ also showed impaired spatial binding. This impairment was unaffected by the duration of the memory delay. Finally, PJ's binding deficits did not generalise across visual dimensions, since he performed normally when recall involved the conjunction of non-spatial features. We conclude that PHC serves a spatially specific binding function in short term memory, and that this function appears to be independent of PHC's role in recall precision.

Methods

PJ: history and clinical assessment

PJ was first seen by one of the authors (CR), four months after he had suffered a cerebrovascular accident. PJ was 45 years old when he developed headaches, visual and mental status changes over the course of a few hours. Two days after the onset of these symptoms, he was admitted to a stroke-unit at a regional hospital. During the admission, he continued to be confused and agitated. The diagnostic work-up revealed bilateral posterior circulation strokes involving the occipito-temporal cortex. No cause for the stroke was identified. PJ had no significant medical history, except for cluster headaches, which responded well to standard treatment.

Upon returning home, he was not able to resume his full-time occupation as an animal breeder, because of difficulties finding his way around the house and farm, where he had moved two years prior. He also relinquished driving, because he could not find his way around familiar streets. He was able to sketch the overall layout of his home, but frequently misidentified rooms and the family resorted to placing signs on internal doors to help him find his way around. His ability to repair equipment around the farm was also diminished, because of difficulty identifying the correct tool in a cluttered environment.

PJ's visual perimetry was formally assessed three and five months following the ischemic injury, with a binocular field test (Esterman, 1982). He showed strict upper quadrantanopias, worse on the left than on the right. There was evidence of partial recovery on the second assessment (see figure S3).

Formal clinical psychometric testing was conducted approximately 6 months following his stroke. The standardised scores are presented in table 1. His general intellectual functioning fell within the average range, as measured with the Wechsler Adult Intelligence scale, fourth edition (WAIS-IV). This was affected negatively by slowed processing speed on visual tasks. He performed similarly on the verbal (Verbal Comprehension Index) and non-verbal scale (Perceptual Reasoning Index) of the WAIS-IV. His expressive and receptive language functions were grossly intact. He did however often require verbal instructions to be repeated. His information-processing speed was in the borderline range on the WAIS-IV. Memory function was significantly impaired for both visual and verbal material. He had difficulties with learning and acquisition of new material and also with delayed recall. Performance was not improved for recognition memory. His errors on a visual memory task were primarily misplacement errors. He demonstrated set-loss errors on a word generation task and also required reminding of rules on a problem-solving task. Performance on executive functioning tasks was mixed; he performed at the expected level on a planning and problem-solving task. His performance on a verbal fluency task was within normal limits. His score on an attention-shifting and inhibition task was in the impaired range of ability. PJ passed on all subtests of object perception from the Visual Object and Space Perception Battery (Warrington and James 1991), except for progressive silhouettes, where he had a raw score of 11, indicating mild impairment. He was also faultless in all subtests of space perception.

PJ was scanned using a research MRI protocol and tested behaviourally at the Bangor University School of Psychology approximately one year and ten months following the ischemic event, when he was 47 years of age. Testing took place on two

consecutive days.

Control Participants

Behavioural comparison: Ten right-handed, healthy male participants were recruited from the local community. Controls were screened for any history of major neuropsychiatric disorders and visual impairments. IQ was measured with the 2-subtest (vocabulary and matrix reasoning) version of the Wechsler Abbreviated Scale of Intelligence (WASI; Wechsler 1999). Table 2 summarises the characteristics of the control group. The mean age was 48.2 years (sd: 6.4), the mean IQ was 101.1 (sd: 7.6) and the mean age leaving school was 16.6 (sd: 0.7). On all these variables, PJ and controls were matched; all p-values were above .095 using a modified t-test (Crawford and Howell 1998).

Anatomical comparison: A convenience sample of 10 healthy male participants was drawn from a Bangor University image register. The mean age was 43.3 years (sd: 4.9).

All participants were compensated for their time and travel expenses. All participants gave written, informed consent prior to initiating any experimental procedure. The testing procedures had been reviewed and approved by the Betsi Cadwaladr University Health Board and the Bangor University School Psychology Ethics committees.

Behavioural testing: overview and material

PJ and controls performed three computer-based behavioural experiments. Testing took place in a dark room; participants sat comfortably, unrestrained, approximately 85cm from an LCD screen (NEC LCD3210). Participants were encouraged to actively scan the display and foveate individual stimuli. Custom-coded Matlab scripts (Mathworks 2014a), using a set of freely available routines designed to facilitate the coding of visual experiments (Brainard 1997), controlled the experiments and generated the displays. Matlab scripts were run on an Apple iMac 10.

Statistical comparison of PJ and controls

We computed the significance of performance differences between PJ and the control group in all experiments using a modified t-test (Crawford and Howell 1998). Where performance was measured with a percentage or ratio, we conducted the t-test on logarithmically transformed values.

Imaging

Imaging – image acquisition and analysis

PJ and the anatomical comparison controls were scanned on a Phillips Achieva 3T MR scanner with a 32-channel head coil. T1 weighted images (TE = 4.32ms; 8° flip angle) were acquired axially with a 0.7mm isotropic voxel-size. PJ's T1 weighted anatomical volume was bias corrected and normalised to the atlas representative MNI152 template using SPM12 (Ashburner and Friston 2003). The mapping included a 12-degrees-of-freedom affine transform followed by a local deformation, computed after the lesion had been masked using a hand-drawn region. The normalised anatomy was obtained by interpolation via a 4^{th} degree B-spline, and resampled using a 0.7mm linear voxel size. Skull stripped anatomy was obtained using a modified version of

FSL's BET, which is optimised for tissue segmentation in the presence of brain pathology (Lutkenhoff et al. 2014). To determine whether PJ's stroke encroached onto perirhinal and entorhinal cortex, probabilistic maps of these regions were superimposed on his brain anatomy (Hindy and Turk-Browne 2016). Lesion boundaries were drawn by a board-certified adult neurologist, using the co-registered T1 and FLAIR images.

Lesion anatomy results

Figure 1 shows axial and coronal slices from the MNI Atlas co-registered T1-weighted scan of PJ's brain. In the left hemisphere the lesion volume is 6.25 cm^3, in the right hemisphere 10.71 cm^3. Figure 1A shows that the ischemic lesions in medial occipitotemporal cortex (mOTC) of the left and right hemisphere lie posterior to the location of entorhinal and perirhinal cortex (marked respectively in red and green), identified in a previous group study (Hindy and Turk-Browne 2016). Figure S1 provides additional anatomical information about the relationship between lesion and entorhinal and perirhinal cortex. The coronal slices in figure 1B demonstrate that the fornix is intact, however sections -23 to -32 suggest hippocampal volume loss on the right. Also, retrosplenial cortex and the adjacent precuneus are spared in both hemispheres. Figure S2 shows sagittal slices through medial brain structures, which highlights the extent of the damage to PHC and lingual gyrus. Given the apparent hippocampal volume loss, we compared PJ's left and right hippocampal volumes to those of the anatomical comparison controls. A stereological procedure was used to estimate hippocampal volumes in all participants (Keller and Roberts 2009). The input images were the T1 weighted brain volumes in native scanner space. A regular cubic grid with a step of 3 pixels was superimposed on coronal slices, with a random

starting position. The senior author, a board-certified neurologist, outlined the hippocampal formation to determine the number of overlaying grid points. The hippocampal formation included the hippocampus, dentate gyrus and subiculum. The anterior border of the hippocampal formation was the alveus, the posterior border was the crux of the fornix. The hippocampal borders were also identified in axial and sagittal slices. The procedure was implemented using ImageJ (Schneider et al. 2012) and a stereology dedicated plugin (Merzin 2008). This analysis indicated that PJ's left (3931mm^3) and right (2530mm^3) hippocampi were not significantly smaller than controls (left: mean = 3561mm^3; $t(9) = 0.516$, $p = 0.618$; right: mean = 3816 mm^3 $t(9) = -1.79$, $p = 0.108$). However, the volumetric difference between the left and right hippocampi was significantly greater for PJ than for controls ($t(9) = 2.641$, $p = 0.027$), suggesting that PJ's right hippocampus may have been atrophied.

Experiment 1: spatial vs. non-spatial binding in working memory

Experiment 1 – Rationale

Primate studies (Malkova and Mishkin 2003; Belcher et al. 2006) have suggested that PHC is involved in remembering locations in close peri-personal space as well as spatial binding in working memory. In this first experiment, we examined visual working memory spatial and feature binding in PJ, a man with PHC lesions, and a group of age-matched controls. On each trial, participants had to remember the colour, shape and location of two objects. After a short delay, participants were cued to recall the colour of one of the objects, identified either by its location on the screen, or by its shape. We reasoned that if human PHC is involved in spatial binding, then PJ's recall performance should be worse than controls, specifically on location trials.

Experiment 1 – Methods

Figure 2A shows a schematic representation of Experiment 1's trial structure. In each trial, an equilateral triangle and a square, whose side lengths were 2.42° and 1.72° respectively, appeared side-to-side in the lower half of the screen, at an eccentricity of 4.25° along the main diagonal, for 2.0s. The shapes were either red, blue or green. A 200ms pattern mask, and then a 2.0s blank screen, followed the sample display. The recall screen contained three coloured rectangles, 1.0° wide and 3.0° high, whose lower edges were aligned 2.5° above the screen center and spaced horizontally 9.0° apart. A bright cross (location cue) or the outline of one of the two shapes (shape cue) identified the target. The location cues, which also included a dark cross, appeared at the locations occupied by the two shapes. The shape cue appeared 3.0° below the screen center. Participants reported the target colour by placing a cursor over the corresponding coloured rectangle and clicking the mouse button. The mouse click prompted the beginning of a new trial, after a 1.0s delay, during which the screen was blank. Participants practiced the task over ten trials and then completed ninety trials, including both shape and location cued recalls. Trial order was randomised, minimising participants' ability to predict whether a shape or location cue would follow the sample display. To ensure that PJ had not forgotten the task instructions, we asked him to describe what he had been doing after each block. In each instance he correctly reported that he had been recalling either the probed shape colour, or the colour at the location of the white cross.

Experiment 1 – Data analysis

We scored trials based on whether participants reported (a) the correct target colour (correct response), (b) the colour of the non-target shape (binding error), or (c) neither

the target nor the non-target colour, i.e., dummy colour (generic error). We then calculated the proportion of binding (BE) and generic errors (GE) for each cue condition ($_{location}$ and $_{shape}$) and compared PJ and the control group's recall accuracy using odds ratios. We computed two odds ratios: the first was the ratio of the proportion of binding errors in location vs. shape cued trials (i.e., [$BE_{location}$ / BE_{shape}]). The second was the ratio of binding errors over generic errors in location vs. shape cued trials (i.e., [$BE_{location}$ / $GE_{location}$] / [BE_{shape} / GE_{shape}]). If a participant's data cells contained zero counts, a value of 0.5 was added to all cells prior to computing the ratios (Gart and Zweifel 1967).

Experiment 1 – Results: impaired spatial binding in visual working memory

The left-hand panels of figures 2B and 2C report the proportion of generic errors following location and shape cues, while the right-hand panels show the proportion of binding errors. PJ made more binding errors when the target was identified by a location than a shape cue ($p < 0.001$; Fisher exact test). PJ was also much more likely to make a binding than a generic error following a location ($p< 0.001$, two-tailed binomial test), but not a shape cue ($p = 0.5$), suggesting that his difficulties did not reflect a problem remembering which colours had been shown. For PJ, the odds ratio of making a binding error in the location vs. shape cue trials was 60.7, which was significantly greater than the control group average of 0.501 (95% CI: [0.23 - 1.06], $t(9) = 3.72$, $p = 0.005$), suggesting that he was much more likely to make a binding error on location than shape cue trials, while controls were modestly more accurate following a location than a shape cue. Moreover, PJ's odds ratio of making a binding rather than a generic error in the location vs shape cued trials was 29.0 which was again significantly greater than the control group average of 0.421 (95% CI: [0.21 -

0.83], t(9) = 3.46, p = 0.007), confirming that he was much more likely to make a binding than a generic error on location rather than shape cued trials, while controls were more likely to make a binding than a generic error on shape rather than location trials.

Experiment 1: Interim discussion

PJ showed a remarkable deficit binding objects to their location in a working memory task. When he reported the colour of one of two objects, he was able to do so accurately for targets cued by their shape. However, when a target was identified by its location, his performance was greatly diminished because of numerous binding errors. Control participants, on the other hand, showed comparable recall accuracy irrespective of the cue type. These findings strongly suggest that PJ's impairment cannot be attributed to either diminished memory for the report feature, i.e. the target's colour, or a binding deficit that generalises across visual dimensions. Rather, PJ shows a binding impairment that is specifically spatial.

Experiment 2: delayed spatial recall

Experiment 2 – Rationale

In the previous experiment, we demonstrated that PJ suffers a specific spatial binding impairment in a working memory task. In experiment 2, we examined whether spatial binding impairments reflect diminished resolution of spatial data in working memory, or rather disruption of spatial binding. To this end we assessed the effects of the duration of the memory delay on both the precision of spatial recall and the proportion of binding errors.

Experiment 2 – Methods

Figure 3A summarises Experiment 2's trial structure. The sample stimulus consisted of three coloured discs, 0.8° in diameter. The discs were red, green and blue, and remained visible for 2.0s. A 1.0s long pattern mask followed the sample. A central colour cue (a 0.3° wide square) appeared either immediately after the pattern mask, or after an additional 4.0s interval, during which only a white central fixation point was visible. The cue identified the target of the same colour. The participants placed the cursor at the recalled target location and clicked the mouse to record their response and initiate the next trial. The location of the discs included the center of the screen and the vertices of a virtual square, at an eccentricity of 6.0°. 2D Gaussian displacement (s.d.= 0.9°) jittered the position of each disc. Each participant completed two blocks of one hundred and twenty trials each.

Experiment 2 – Data analysis

First, we identified trials in which participants had made a binding error, i.e. when the recalled position was closer to the one of the non-target items than the target, and the distance from the non-target item was no greater than half the minimum distance between canonical locations, i.e. 3.0° (Pertzov et al. 2013). After tabulating and removing binding errors, we estimated recall accuracy and precision. Accuracy reflects how close a participant's average reported location is to the true target position. Precision reflects the magnitude of trial-to-trial deviations from a participant's average reported location. Accuracy is diminished by systematic errors, which depend on factors such as display size and memory load (Katshu and d'Avossa 2014), while precision is thought to reflect the resolution of spatial memory (Bays et al. 2009). These two variables were computed using linear regressions. We computed

two regressions whose dependent variables were the azimuth and elevation of the reported target location, respectively. The regressors in each case included a constant and the target's azimuth and elevation. The results of the regression analysis were used to estimate the systematic biases reporting the target location. The scaling factor was the divergence of the error field, which we previously found to be the main linear component of the systematic error (Katshu and d'Avossa 2014). We quantified recall precision using the standard deviation of the residuals from the model fits. The variance and standard deviations of the variable errors were computed using the same procedure employed in a previous study (Katshu and d'Avossa 2014), and averaged over azimuth and elevation. Precision changes between short and long delays were quantified using an efficiency measure, namely a ratio whose numerator was the recall variance following 1.0s delays and denominator was recall variance following 5.0s delays.

Experiment 2 – Results: recall precision, but not binding errors, affected by memory delay

PJ made more binding errors than controls, following both 1.0s and 5.0s delays. Otherwise, both PJ and controls performed similarly in terms of accuracy and precision.

The proportion of binding errors are shown in the left-hand panels of figure 3B and 3C. Overall, PJ made a binding error on 9.44% of trials, which was significantly greater than the control group average of 3.21% (95% CI: [2.24 - 4.18]; $t(9) = 4.02$; $p = 0.003$). Increasing the duration of the memory delay had no effect on the proportion of PJ's relative binding errors; PJ's odds ratio for making a binding error following

1.0s vs. 5.0s delays was 1.27, which was not significantly different to the control group average of 1.0 (95% CI: [0.72 - 1.38]; $t(9) = 0.462$; $p = 0.655$), and suggested a non-significant tendency for more binding errors following short than long memory delays. Further, 40% (6/15) of PJ's binding errors on short delay trials, and 50% (6/12) of his binding errors on long delay trials, occurred when the target appeared in the upper portion of the screen; a goodness of fit test reported that his binding errors were not biased toward the target appearing in either the upper or lower half of the screen following either delay (χ^2 (3) = 1, p = .801). We can therefore conclude that his binding issues are unlikely due to his upper visual field deficit impacting the encoding of the entire sample stimulus.

Both PJ and controls showed systematic distortions. Following both short and long memory delays, PJ reported targets displaced leftward (1.0s: -0.24°; 5.0s: -0.23°) and upward (1.0s: 0.15°; 5.0s: 0.09°). In contrast, controls' group mean displacement was rightward (1.0s: 0.09°, 95% CI: [-0.09 – 0.26]; 5.0s: 0.07°, 95% CI: [-0.12 – 0.27];) and downward (1.0s: -0.37°, 95% CI: [-0.55 – -0.19]; 5.0s: -0.28°, 95% CI: [-0.45 – -0.11]). However, PJ's displacements were not significantly different from controls for both delays (all p-values > 0.100). PJ also tended to overestimate the position of targets relative to the screen center, indicated by an error divergence of 0.04 following 1.0s delays and 0.16 following 5.0s delays. In contrast, controls underestimated targets relative to the screen center, as indicated by a group average error divergence of -0.26 (95% CI: [-0.36 – -0.15]) following 1.0s delays and -0.29 (95% CI: [-0.41 – -0.16]) following 5.0s delays. However, PJ and controls did not differ significantly (both p-values > 0.055).

Recall precision data are summarised in the right-hand panel of figure 3B and 3C. In contrast to binding errors, increasing the delay had a significant effect on recall precision. PJ's error standard deviation was 1.33° following 1.0s delays, which was not statistically different from the control group average of 1.01° (95% CI: [0.91 – 1.10]; t(9) = 2.11; p = 0.064). PJ's error standard deviation following 5.0s delays (1.78°) was statistically larger than the control group average of 1.18° (95% CI: [1.09 – 1.27]; t(9) = 4.23; p = 0.002). However, PJ's efficiency after a 5.0s delay compared to a 1.0s delay was 0.56, which was not significantly smaller than the control group average of 0.73 (95% CI: [0.65 – 0.82]; t(9) = -1.37; p = 0.203).

Experiment 2: Interim discussion

The experiment yielded a number of findings. First PJ made more binding errors than controls, confirming that he exhibited an impairment of spatial binding using a task in which the target location was the report rather than the cue variable. Secondly, following 1.0s delay the precision recalling the target location was not appreciably different between PJ and controls, suggesting that his binding impairment did not reflect a problem recalling the target location precisely. Moreover, while increasing the memory delay did not increase the proportion of binding errors, it did significantly diminish both PJ and controls' spatial recall precision, providing additional evidence that recall precision did not account for binding errors. In summary, PJ shows frequent binding errors, but spatial recall precision which is comparable to that of controls. Crucially, changing the duration of the memory delay produces dissociable effects on recall precision and binding.

Experiment 3: centroid estimation

Experiment 3 – Rationale

In experiment 3 we ascertained whether PJ's diminished recall of a target position may reflect a sensory impairment. While this seems unlikely given the finding that PJ's recall precision was not significantly diminished compared to controls (with 1.0s delay), it was important to establish the extent to which sensory difficulties may have limited his performance. We therefore assessed participants' spatial accuracy and precision in a perceptual task.

Experiment 3 – Methods

This experiment assessed participants' ability to localise the centroid, namely the average location, of three white discs. The discs' diameter was 0.5° (see figure 4A for a schematic representation of the trial structure). The discs remained visible until participants had positioned a crosshair shaped cursor at the desired location and clicked the mouse. Following a blank, 1.0s-long interval, a novel set of discs appeared and the procedure was repeated. Discs could occupy any of seven canonical locations. These included the screen center and the vertices of a virtual concentric hexagon, with a side length of 6.87°. All permutations of three out of seven canonical target locations, less any resulting in a collinear configuration, were used as sample arrays. Each possible permutation appeared twice, for a total of sixty-four trials. A pseudorandom, zero mean, circular Gaussian distribution, with a standard deviation of 0.6°, was used to jitter each disc's position independently. Prior to testing, instructions were read to the participants. The centroid was defined as the point in space where the triangle, whose vertices coincided with the discs' locations, would balance in the horizontal plane (Baud-Bovy and Soechting 2001). One of the experimenters also provided a visual demonstration, using a cut-out triangular shape.

Prior to testing, participants completed twenty-five practice trials. At the end of each practice trial, the reported and actual positions of the centroid were shown for 2.0s.

Experiment 3 – Data analysis

We estimated the systematic and variable error of participants' centroid estimations, by fitting a linear model to the azimuth and elevation of the reported centroid location. The model regressors included a constant and the centroid azimuth and elevation. Two metrics were used to characterise the systematic error: 1) the constant displacement, that is the tendency to report the centroid above, below, right or left of its true location, and 2) scaling factor, measuring the linear relationship between reported and actual centroid positions. These are, respectively, the estimated intercept and beta parameters of the linear model. We computed precision as the standard deviation of the variable error, i.e., residuals from the model, using the same methods used in Experiment 2.

Experiment 3 – Results: accuracy and precision of centroid estimation

The left-hand panels of figure 4B and 4C illustrate the direction of systematic biases in centroid estimates. PJ and controls respectively reported the centroid -0.07° and -0.10° (95% CI: [-0.15° – -0.04°]) left of its veridical position, suggesting that both showed a similarly small leftward bias, ($t(9) = 0.322$, $p = 0.755$). However, PJ reported the centroid 0.56° above its veridical position. This bias was significantly larger than controls, who showed a group average upward bias of 0.06° (95% CI: [-0.02° – 0.14°]; $t(9) = 3.69$, $p = 0.005$). The middle panel of figure 4B and 4C summarise the linear scaling for centroid estimates. PJ varied the reported centroid azimuth by a factor of 0.97, and elevation by a factor of 1.00, in both cases reflecting

an almost perfect linear relationship between reported an actual centroid positions. These values were comparable to those shown by controls, namely 0.99 for azimuth (95% CI: [0.94 – 1.03]; t(9) = -0.263, p = 0.799), and 0.97 for elevation (95%CI: [0.93 – 1.01]; t(9) = 0.443, p = 0.668). Finally, PJ's azimuth variable error standard deviation, 0.67°, was not significantly different from the control average of 0.69° (95%CI = [0.56° - 0.82°]; t(9) = -0.091, p = 0.931), nor was his elevation variable error standard deviation, 0.77°, significantly different from the control average of 0.59° (95%CI = [0.47° - 0.70°]; t(9) = 0.925, p = 0.380), suggesting that both the vertical and horizontal precision of his centroid judgements was relatively spared.

Experiment 3 – Interim discussion

PJ showed a strong tendency to report the centroid above its true location. This probably represents a compensatory strategy for his upper visual field defect. In fact, hemianopic patients display a bias toward their blind field when judging the midpoint of horizontal line (Barton and Black 1998; Kerkhoff and Buchers 2008). However, both PJs accuracy and precision estimating the centroid position were within the control group's range. We conclude that aside from compensatory visual defect biases, PJ's ability to localise perceptually is largely spared and unlikely to account for his diminished recall precision.

Discussion

We tested a middle-aged man (PJ) with bilateral mOTC strokes involving the PHC. Acutely, PJ had developed a derangement of attention and short-term memory (Horenstein et al. 1967; Medina et al. 1977; Shih et al. 2007). At the time of testing, PJ was no longer delirious, but continued to have difficulties with his memory as well as navigating familiar environments. The latter is a form of spatial disorientation previously attributed to PHC lesions in humans (Zola-Morgan et al. 1989; Epstein et al. 2001). Animal studies have demonstrated additional deficits in spatial working memory following PHC lesions in non-human primates (Malkova and Mishkin 2003; Bachevalier and Nemanic 2008). Whether the same deficits characterise human patients with PHC lesions is not yet known.

We found that PJ had a profound deficit binding an object to its location in a working memory task. When he recalled the colour of one of two objects, after a short memory delay, he could accurately do so when the target was cued by its shape. However, when the target was cued by its location, his accuracy was greatly diminished because he made numerous binding errors, frequently reporting the colour of the non-target item instead of the colour of the target. Control participants, on the other hand, were accurate whether the target was identified by the location or shape cue. These findings strongly suggest that PJ was impaired only when using a location cue and that this impairment could not be attributed to either diminished memory for the report feature, i.e. the target's colour, or a binding deficit that generalises across spatial and non-spatial visual dimensions. According to a recent study, generalised binding difficulties may instead characterise recall performance in individuals with autoimmune temporal encephalitis, which mainly affects the hippocampal formation (Pertzov et al. 2013).

Some animal and imaging studies have indeed shown that both anterior PHC and hippocampus contribute to object-in-place associations in short-term memory (Milner et al. 1997; Bachevalier and Nemanic 2008). However, animal data suggest that hippocampal involvement in spatial binding is restricted to tasks where spatial relations are incidentally encoded (Bachevalier and Nemanic 2008). These findings, together with ours, suggest that in tasks where spatial information is intentionally encoded and recalled, the role of PHC goes beyond simply providing spatial data to the hippocampus, where general purpose processes bind visual features in working memory. Moreover, our findings confirm that binding in visual working memory is liable to be disrupted by focal brain lesions (Gorgoraptis et al. 2011), supporting the idea that it is a neural function independent from those underpinning the representations of individual features (Wheeler and Treisman 2002; Smyrnis et al. 2005).

Binding errors do not reflect the resolution of spatial information

When PJ reported the location of one of three objects held in memory he erroneously reported the location of one of the non-target items more frequently than controls. This finding suggests that PJ had difficulties with spatial binding, whether space was the cue or report dimension. One might argue that PJ's spatial binding impairment simply reflects degraded spatial representations. In other words, diminished ability recalling the location of an object might explain his difficulties using spatial information to identify targets in memory. However, this hypothesis is not supported by our data. PJ was able to estimate the centroid of simple dot configurations as precisely as controls, indicating that despite the presence of an upper visual field

defect, the spatial resolution of visual data was not prominently affected in this perceptual task. Moreover, PJ's precision recalling the location of visual targets was not appreciably different from that of controls, even though his proportion of spatial binding errors was much greater. Finally, binding errors did not become more frequent when the delay interval was increased, although the precision of spatial recall did decrease. We conclude that binding errors do not reflect the temporal decay of a memory trace, contrary to previous suggestions (Zhang and Luck 2009). Moreover, our findings are consistent with observations that binding errors are not affected by the duration of the memory delay in either patients with hippocampal pathology (Pertzov et al. 2013) or healthy controls (Gorgoraptis et al. 2011), although whether binding errors may be effected by longer (e.g., >20.0s) delays remains to be established. Finally, varying the spatial memory demands at the time of recall in a spatial version of the Sternberg working memory task does not change the likelihood of committing a binding error, confirming that binding errors do not reflect confusion among features of the probe dimension (Smyrnis et al. 2005). Taken together, the available evidence in healthy controls and patients instead suggests that binding errors reflect interference with early processes, engaged at the time when visual information is encoded in working memory. However, a recent high-resolution fMRI study has suggested that load dependent signals in PHC during the delay period of a match-to-sample-task may reflect on-going binding processes (Schon et al. 2016).

Delays affect the precision of spatial recall

PJ's spatial recall precision was similar to that of controls when the memory delay lasted 1.0s. When the memory delay was 5.0s long, both he and controls suffered a decrement in recall precision. These are not entirely novel findings. Recall precision

is known to decrease with longer memory delays in healthy controls (Sheth and Shimojo 2001; Zhang and Luck 2009). Moreover, recall precision disproportionally decreases in patients with PHC lesions, although significantly so only following memory delays greater than 20s (Ploner et al. 2000). This finding is in keeping with our own: recall efficiency following 5.0s vs 1.0s delays was lower in PJ than in controls, however this difference was not significant. Combined, these data are consistent with the idea that following PHC lesions, spatial recall precision decays more quickly than in healthy controls, as opposed to declining abruptly. More generally, our findings are in keeping with the view that spatial recall draws information from a limited capacity resource (Bays et al. 2009), whose resolution diminishes over time. Therefore, delay dependent changes in spatial recall precision most likely reflect a limited ability to maintain information in working memory rather than impaired encoding, in contrast to the binding deficits discussed above. Finally, PJ's performance in our experiments is consistent with his neuropsychological profile, which is principally characterised by impairment on various memory tasks, including those that do not have a spatial binding component, such as the Logical Memory test and the Rey Auditory Verbal Learning Test. However we do not yet know the extent to which diminished recall precision and spatial binding account for the broad memory deficits observed following lesions to PHC.

Could the hippocampus be the site for short term memory spatial binding?

In the present study we identified impairments resulting from focal lesions to PHC, and found a spatial binding deficit in short term memory. Our data cannot rule out the possibility that binding takes place outside PHC, for example, in the hippocampus. Indeed, comparison of hippocampal volumes in PJ and age and gender matched

controls suggest hippocampal atrophy in PJ. Lateralised hippocampal atrophy commonly follows distal, ipsilateral stroke, even in young patients unlikely to harbour neurodegenerative processes (Schaapsmeerders et al. 2015a, 2015b), suggesting that the hippocampus may be particularly vulnerable to the effects of deafferentation. Pj's hippocampal atrophy raises the possibility that spatial binding deficits reflect diminished function within the hippocampus. Our data cannot refute this alternative hypothesis. As mentioned in the introduction, previous studies in patients with inflammatory and anoxic damage involving the hippocampus (e.g. Pertzov et al. 2013; Watson et al. 2013; Yee et al. 2014) have also demonstrated spatial binding impairments, lending support to the hippocampus' role in feature binding. Nonetheless, the specific spatial nature of PJ's binding impairment, which did not generalise to other visual dimensions (i.e., shape), is inconsistent with the proposal that the hippocampus provides a general purpose binding mechanism. Therefore, we conclude that spatial binding is either carried out in hippocampus, using inputs from PHC, or that PHC itself initiates spatial binding processes.

Concluding remarks

This study provides novel information on the role of MTL, by showing that a man with a lesion involving PHC, hippocampal atrophy, but spared PRC, has a selective deficit in short term spatial binding. This deficit is not explained by diminished resolution of spatial information. Our findings are consistent with the idea that spatial binding processes in short term memory may be initiated in the PHC even before visual information reaches the hippocampus.

Acknowledgments

This work was supported in part by the Biotechnology and Biological Sciences Research Council grant BB/1007091/1. The authors thank Paul Mullins for his assistance with MRI data acquisition, and for providing the anatomical control data.

References

Aggleton JP. 1992. The functional effects of amygdala lesions in humans: A comparison with findings from monkeys. New York (NY): Wiley-Liss.

Ashburner J, Friston KJ. 2003. Spatial normalization using basis functions. In: Frackowiak RS, Friston KJ, Frith CD, Dolan RJ, Price CJ, Ashburner J, Penny WD, Zeki S, editors. Human brain function. Oxford: Academic Press. p. 655-672.

Bachevalier J, Nemanic S. 2008. Memory for spatial location and object-place associations are differently processed by the hippocampal formation, parahippocampal areas TH/TF and perirhinal cortex. Hippocampus. 18(1):64-80.

Barker GR, Warburton EC. 2011. When is the hippocampus involved in recognition memory? J Neurosci. 31(29):10721-10731.

Barton JJ, Black SE. 1998. Line bisection in hemianopia. J Neurol Neurosurg Psychiatry. 64(5):660-662.

Baud-Bovy G, Soechting J. 2001. Visual localization of the center of mass of compact, asymmetric, two-dimensional shapes. J Exp Psychol Hum Percept Perform. 27(3):692-706.

Bays PM, Catalao RF, Husain M. 2009. The precision of visual working memory is

set by allocation of a shared resource. J Vision. 9(10):7-7.

Belcher AM, Harrington, RA, Malkova, L, Mishkin, M. 2006. Effects of hippocampal lesions on the monkey's ability to learn large sets of object-place associations. Hippocampus. 16(4):361-367.

Brainard DH. 1997. The psychophysics toolbox. Spatial vision. 10:433-436.

Burwell RD, Amaral DG. 1998. Perirhinal and postrhinal cortices of the rat: interconnectivity and connections with the entorhinal cortex. J Comp Neurol. 391(3):293-321.

Corkin S. 1984, June. Lasting consequences of bilateral medial temporal lobectomy: Clinical course and experimental findings in HM. Semin Neurol. 4(2):249-259.

Corkin S, Amaral DG, González RG, Johnson KA, Hyman, BT. 1997. HM's medial temporal lobe lesion: findings from magnetic resonance imaging. J Neurosci. 17(10):3964-3979.

Crawford JR, Howell DC. 1998. Comparing an individual's test score against norms derived from small samples. Clin Neuropsychol. 12(4):482-486.

Davachi L, Goldman-Rakic PS. 2001. Primate rhinal cortex participates in both visual recognition and working memory tasks: functional mapping with 2-DG. J Neurophys. 85(6):2590-2601.

Deacon RM, Bannerman DM, Kirby BP, Croucher A, Rawlins JNP. 2002. Effects of cytotoxic hippocampal lesions in mice on a cognitive test battery. Behav Brain Res. 133(1):57-68.

Diana RA, Yonelinas AP, Ranganath C. 2007. Imaging recollection and familiarity in the medial temporal lobe: a three-component model. Trends Cogn Sci. 11(9):379-386.

Eichenbaum H, Yonelinas AR, Ranganath C. 2007. The medial temporal lobe and recognition memory. Annu Rev Neurosci. 30:123.

Epstein R, DeYoe EA, Press DZ, Rosen AC, Kanwisher N. 2001. Neuropsychological evidence for a topographical learning mechanism in parahippocampal cortex. Cognitive Neuropsychol. 18(6):481-508.

Esterman B. (1982). Functional scoring of the binocular field. Ophthalmology. 89:1226-1234.

Friedman HR, Goldman-Rakic PS. 1988. Activation of the hippocampus and dentate gyrus by working-memory: a 2-deoxyglucose study of behaving rhesus monkeys. J Neurosci. 8(12):4693-4706.

Gorgoraptis N, Catalao RF, Bays PM, Husain M. 2011. Dynamic updating of working memory resources for visual objects. J Neurosci. 31(23):8502-8511.

Graham KS, Barense MD, Lee AC. 2010. Going beyond LTM in the MTL: a synthesis of neuropsychological and neuroimaging findings on the role of the medial temporal lobe in memory and perception. Neuropsychologia. 48(4):831-853.

Habib M, Sirigu A. 1987. Pure topographical disorientation: a definition and anatomical basis. Cortex. 23(1):73-85.

Hindy NC, Turk-Browne NB. 2016. Action-based learning of multistate objects in the medial temporal lobe. Cereb Cortex. 26(5):1853-1865.

Holdstock JS, Shaw C, Aggleton JP. 1995. The performance of amnesic subjects on tests of delayed matching-to-sample and delayed matching-to-position. Neuropsychologia. 33(12):1583-1596.

Holdstock JS, Mayes AR, Roberts N, Cezayirli E, Isaac CL, O'Reilly RC, Norman KA. 2002. Under what conditions is recognition spared relative to recall after selective hippocampal damage in humans?. Hippocampus. 12(3):341-351.

Horenstein S, Chamberlin W, Conomy J. 1967. Infarction of the fusiform and calcarine regions: agitated delirium and hemianopia. T Am Neurol Assoc. 92:85.

Jeneson A, Mauldin KN, Squire LR. 2010. Intact working memory for relational

information after medial temporal lobe damage. J Neurosci. 30(41):13624-13629.

Katshu MZUH, d'Avossa G. 2014. Fine-grained, local maps and coarse, global representations support human spatial working memory. PloS one. 9(9):e107969.

Keller SS, Roberts N. 2009. Measurement of brain volume using MRI: software, techniques, choices and prerequisites. J Anthropol Sci. 87:127-51.

Kerkhoff G, Bucher L. 2008. Line bisection as an early method to assess homonymous hemianopia. Cortex. 44(2):200-205.

Libby LA, Hannula DE, Ranganath C. 2014. Medial temporal lobe coding of item and spatial information during relational binding in working memory. J Neurosci. 34(43):14233-14242.

Luck D, Danion JM, Marrer C, Pham BT, Gounot D, Foucher J. 2010. The right parahippocampal gyrus contributes to the formation and maintenance of bound information in working memory. Brain Cognition. 72(2):255-263.

Lutkenhoff ES, Rosenberg M, Chiang J, Zhang K, Pickard JD, Owen AM, Monti MM. 2014. Optimized brain extraction for pathological brains (optiBET). PLoS One. 9(12):e115551.

Malkova L. Mishkin M. 2003. One-trial memory for object-place associations after separate lesions of hippocampus and posterior parahippocampal region in the monkey. J Neurosci. 23(5):1956-1965.

Medina JL, Chokroverty S, Rubino FA. 1977. Syndrome of agitated delirium and visual impairment: a manifestation of medial temporo-occipital infarction. J Neurol Neurosurg Psychiatry. 40(9):861-864.

Merzin M. 2008. Applying stereological method in radiology. Volume measurement. Bachelor's thesis. University of Tartu.

Olson IR, Page K, Moore KS, Chatterjee A, Verfaellie M. 2006a. Working memory for conjunctions relies on the medial temporal lobe. J Neurosci. 26(17):4596-4601.

Olson IR, Moore KS, Stark M, Chatterjee A. 2006b. Visual working memory is impaired when the medial temporal lobe is damaged. J Cog Neurosci. 18(7):1087-1097.

Owen AM, Sahakian BJ, Semple J, Polkey CE, Robbins TW. 1995. Visuo-spatial short-term recognition memory and learning after temporal lobe excisions, frontal lobe excisions or amygdalo-hippocampectomy in man. Neuropsychologia. 33(1):1-24.

Pertzov Y, Miller TD, Gorgoraptis N, Caine D, Schott JM, Butler C, Husain M. 2013.

Binding deficits in memory following medial temporal lobe damage in patients with voltage-gated potassium channel complex antibody-associated limbic encephalitis. Brain. awt129.

Ploner CJ, Gaymard BM, Rivaud-Péchoux S, Baulac M, Clémenceau S, Samson S, Pierrot-Deseilligny C. 2000. Lesions affecting the parahippocampal cortex yield spatial memory deficits in humans. Cereb Cortex. 10(12):1211-1216.

Ranganath C, Blumenfeld RS. 2005. Doubts about double dissociations between short-and long-term memory. Trends Cogn Sci. 9(8):374-380.

Reisel D, Bannerman DM, Schmitt WB, Deacon RM, Flint J, Borchardt T, Seeburg PH, Rawlins JNP. 2002. Spatial memory dissociations in mice lacking GluR1. Nat Neurosci. 5(9):868-873.

Schaapsmeerders P, van Uden IW, Tuladhar AM, Maaijwee NA, van Dijk EJ, Rutten-Jacobs LC, Arntz RM, Schoonderwaldt HC, Dorresteijn LD, de Leeuw FE, Kessels RP. 2015. Ipsilateral hippocampal atrophy is associated with long‐term memory dysfunction after ischemic stroke in young adults. Hum Brain Mapp. 36(7):2432-2442.

Schaapsmeerders P, Tuladhar AM, Maaijwee NA, Rutten-Jacobs LC, Arntz RM, Schoonderwaldt HC, Dorresteijn LD, van Dijk EJ, Kessels RP, de Leeuw FE. 2015. Lower ipsilateral hippocampal integrity after ischemic stroke in young adults: a long-term follow-up study. PloS One. 10(10):p.e0139772.

Schneider CA, Rasband WS, Eliceiri KW. 2012. NIH Image to ImageJ: 25 years of image analysis. Nat Methods. 9:671-675.

Schon K, Newmark RE, Ross RS, Stern CE. 2016. A working memory buffer in parahippocampal regions: evidence from a load effect during the delay period. Cereb Cortex. 2016. 26(5):1965-74.

Scoville WB, Milner B. 1957. Loss of recent memory after bilateral hippocampal lesions. J Neurol Neurosurg Psychiatry. 20(1):11-21.

Sheth BR, Shimojo S. 2001. Compression of space in visual memory. Vision Res. 41(3):329-341.

Shih H, Huang W, Liu C, Tsai T, Lu C, Lu M, Chen P, Tseng C, Jou S, Tsai C, Lee CC. 2007. Confusion or delirium in patients with posterior cerebral arterial infarction. Acta Neurol Taiwanica. 16(3):136-142.

Smyrnis N, d'Avossa G, Theleritis C, Mantas A, Ozcan A, Evdokimidis I. 2005. Parallel processing of spatial and serial order information before moving to a remembered target. J Neurophysiol. 93(6):3703-3708.

Suzuki WA, Miller EK, Desimone R. 1997. Object and place memory in the macaque entorhinal cortex. J Neurophysiol. 78(2):1062-1081.

Suzuki WL, Amaral DG. 1994. Perirhinal and parahippocampal cortices of the macaque monkey: cortical afferents. J Comp Neurol. 350(4):497-533.

Warrington EK, James M. 1991. The visual object and space perception battery. Bury St Edmunds (United Kingdom): Thames Valley Test Company.

Watson PD, Voss JL, Warren DE, Tranel D, Cohen NJ. 2013. Spatial reconstruction by patients with hippocampal damage is dominated by relational memory errors. Hippocampus. 23(7):570-580.

Wechsler D. 1999. Wechsler abbreviated scale of intelligence. Psychological Corporation.

Wheeler ME, Treisman AM. 2002. Binding in short-term visual memory. J Exp Psychol Gen. 131(1):48-64.

Yee LT, Hannula DE, Tranel D, Cohen NJ. 2014. Short-term retention of relational memory in amnesia revisited: accurate performance depends on hippocampal integrity. Front Human Neurosci. 8(16).

Yonelinas AP. 2013. The hippocampus supports high-resolution binding in the service of perception, working memory and long-term memory. Behav Brain Res. 254:34-44.

Zhang W, Luck SJ. 2009. Sudden death and gradual decay in visual working memory.

Psychol Sci. 20(4):423-428.

Zola-Morgan S, Squire LR, Amaral DG, Suzuki WA. 1989. Lesions of perirhinal and parahippocampal cortex that spare the amygdala and hippocampal formation produce severe memory impairment. J Neurosci. 9(12):4355-4370.

Tables

Neurocognitive domain / Test / Subtest	Raw score	Standard/Z Score	Percentile
Intellectual Functioning			
Wechsler Intelligence Scale - IV			
Full Scale IQ		87	19
Verbal Comprehension Index		96	39
Perceptual Reasoning Index		90	25
Working Memory Index		92	25
Processing Speed Index		79	8
Vocabulary		9	37
Similarities		9	37
Information		10	50
Block Design		9	37
Matrix Reasoning		5	5
Visual Puzzles		11	63
Digit Span		9	37
Arithmetic		8	25
Symbol Search		7	16
Coding		5	5
Learning and Memory			
Wechsler Memory Scale			
Logical Memory I	11/75	2	0.4
Logical Memory II	4/50	3	1
Visual Reproduction I	56	4	2

Visual Reproduction II	13	5	5
Auditory Verbal Learning Test			
Trial I	3	-2	2
Trial II	4	-2.33	1
Trial III	5	-2	2
Trial IV	8	-1.15	13
Trial V	5	-3.31	1
List B	4	-1.11	13
Trial VI	3	-2.2	2
Delayed Recall	1	-2.54	1
Recognition	1	-4.3	1
Rey Complex Figure Test			
Copy	36	1.38	92
30 minute recall	1.5	-2.25	< 1
Benton Visual Retention Test			
Correct score	3	-2.69	< 1
Error score	13	-3.35	< 1
Attention/Executive Function			
Trail Making Test			
Part A	72 sec	-4.05	< 1
Part B	131 sec	-4.66	< 1
D-K Executive Function System			
Verbal Fluency Test			

Letter Fluency	25	6	9
Category Fluency	39	10	50
Tower Test			
Total Achievement Score	16	10	50
Stroop Test			
Colour task	112		
Colour-word task	38		> 2

Object recognition and Space Perception

The Visual Object and Space Perception Battery	
Object Perception	
Screening Test	20/20 (Pass)
Incomplete Letters	19/20 (Pass)
Silhouettes	19/30 (Pass)
Object Decision	17/20 (Pass)
Progressive Silhouettes	11 (Fail)
Space Perception	
Dot Counting	10/10 (Pass)
Position Discrimination	20/20 (Pass)
Number Location	10/10 (Pass)
Cube Analysis	10/10 (Pass)

Table 1. Summary of PJ's neuropsychometric performance six months after stroke.

Gender	Handed	Age	IQ	Age Leaving School
M	Right	51	106	18
M	Right	43	111	16
M	Right	45	99	16
M	Right	61	103	17
M	Right	39	109	18
M	Right	47	90	16
M	Right	53	88	16
M	Right	46	104	17
M	Right	53	97	16
M	Right	44	104	16
	Mean	48.2	101.1	16.6
	SD	6.4	7.6	0.8

Table 2. Control group demographics and IQ

Captions

Figure 1. Lesion anatomy. T1 weighted, MNI atlas registered axial (panel A) and coronal (panel B) slices are displayed in neurological coordinates, and illustrate the extent of ischemic damage in the left and right mOTC. In panel A, the axial slices also highlight the location of entorhinal and perirhinal cortex, in red and green respectively. These regions lay anteriorly and laterally to the boundaries of the ischemic lesions. In panel B, coronal slices highlight parahippocampal and hippocampal structures, including the fornix. The ischemic lesions lay inferiorly and posteriorly to the hippocampus and spare the fornix and the retrosplenial cingulate cortex.

Figure 2. Spatial vs. non-spatial binding in working memory. Panel A shows the trial structure. The sample display for all participants (including PJ) contained a square and a triangle, placed side by side in the bottom half of the screen. The two objects were red, blue or green and never had the same colour. After a brief pattern mask and blank delay, three vertical coloured bars appeared as well as a cursor, which the participant used to report the colour of the memory target. In shape trials, targets were identified by a probe whose outline matched the target shape. In location trials, the location of targets were identified by a white cross. Panel B shows each individual participants' error rate on a greyscale, with lighter colours representing a higher proportion of errors; the left panel shows generic errors, the right panel shows binding errors. On each panel, the upper row shows errors following shape probes, while the lower row shows errors following location probes, for PJ (blue outline) and each of the controls (red outline). Panel C shows PJ's and the group averaged proportion of generic and binding errors. Error bars are standard error of the mean.

Figure 3. Delayed spatial recall. Panel A shows the structure of immediate and delayed, spatial recall trials. The sample display for all participants (including PJ) contained three coloured discs, which could appear in both the upper and lower portion of the screen. The participants had to reproduce the position of one of the discs (the target) using a mouse cursor after either a 1.0s pattern mask or an additional 4.0s delay. The target was identified by its colour, indicated by a visual probe displayed at the center of the screen. Panel B (left) shows PJ's (blue outline) and controls' (red outline) individual percentage of binding errors on a greyscale, following 1.0s (upper row) and 5.0s (lower row) delays, with lighter colours representing a higher proportion of errors. Panel B (right) shows recall precision (95% error ellipses) in 1.0s and 5.0s delayed recall trials for PJ (blue) and controls (red). Panel C shows PJ's and the group averaged proportion of binding errors and precision. Error bars are standard error of the mean.

Figure 4. Centroid estimation. Panel A shows the trial structure. The participants placed a cursor at the centroid of the configuration formed by three bright discs. The discs remained visible until the participant made a response by clicking the mouse. Panel B shows each participant's constant displacement (arrow vectors), scaling (diamond plot) and precision (uncertainty ellipses) in locating the centroid. The length of the diamond plot's hemi-axes corresponds to 1.0 scaling factor. Panel C shows PJ's and group averaged values of the constant displacement and scaling factor, separately for azimuth (X) and elevation (Y). The precision measure shown is the square root of the mean error variance for azimuth and elevation. Error bars in all cases are standard error of the mean.

976

977

Human parahippocampal cortex supports spatial binding in visual working memory

Neil Michael Dundon[1,2], Mohammad Zia Ul Haq Katshu[3], Bronson Harry[4], Daniel Roberts[5], E. Charles Leek[1,6], Paul Downing[1], Ayelet Sapir[1], Craig Roberts[7], Giovanni d'Avossa[1,7]

[1]Bangor University, School of Psychology; [2]University of Freiburg, Department of Child and Adolescent Psychiatry, Psychotherapy and Psychosomatics; [3]University of Nottingham Faculty of Medicine and Health Sciences, Division of Psychiatry and Applied Psychology; [4]Western Sydney University Bankstown campus, The MARCS Institute for Brain, Behaviour and Development; [5]Liverpool John Moores University Faculty of Science, School of Natural Sciences and Psychology; [6]Universite Grenoble Alpes, Laboratoire de Psychologie et NeuroCognition (LPNC); [7]Betsi Cadwaladr University Health Board, North Wales Brain Injury Service

Corresponding author:

Giovanni d'Avossa**,**

School of Psychology - Brigantia Building,

Bangor University,

Bangor, LL572AS,

Gwynedd, UK.

Tel: +441248388801 / Fax: +441248382599

Email: g.davossa@bangor.ac.uk

Running title: Human PHC supports spatial binding

Abstract

Studies investigating the functional organisation of the medial temporal lobe (MTL) suggest that parahippocampal cortex (PHC) generates representations of spatial and contextual information used by the hippocampus in the formation of episodic memories. However, evidence from animal studies also implicates PHC in spatial binding of visual information held in short term, working memory. Here we examined a 46-year-old man (PJ), after he had recovered from bilateral medial occipitotemporal cortex strokes resulting in ischemic lesions of PHC and hippocampal atrophy, and a group of age-matched healthy controls. When recalling the colour of one of two objects, PJ misidentified the target when cued by its location, but not shape. When recalling the position of one of three objects, he frequently misidentified the target, which was cued by its colour. Increasing the duration of the memory delay had no impact on the proportion of binding errors, but did significantly worsen recall precision in both PJ and controls. We conclude that PHC may play a crucial role in spatial binding during encoding of visual information in working memory.

Keywords: Feature binding; Medial temporal lobe; Parahippocampal cortex; Spatial Memory; Visual working memory

Introduction

The medial temporal lobe (MTL) comprises the hippocampus and parahippocampal regions, i.e., entorhinal cortex, perirhinal cortex (PRC) and parahippocampal cortex (PHC). These structures play a prominent role in episodic memory, as evidenced by the dense anterograde amnesia, which follows damage to MTL (Scoville and Milner 1957; Corkin 1984; Corkin et al. 1997). Modular accounts of MTL function have suggested that the hippocampus synthesises episodic memories by binding information about the identity and location of objects carried respectively by two different streams (Eichenbaum et al. 2007; Diana et al. 2007).

MTL structures have also been implicated in short term memory processes (Ranganath and Blumenfeld 2005; Graham et al. 2010; Yonelinas, 2013). First, animal models have pointed to specific molecular mechanisms in the mammalian MTL dedicated to the storage of short term memories, and separate from those involved in long term memory (Deacon et al. 2002; Reisel et al. 2002). Single unit recordings and lesion studies in non-human primates have further demonstrated that the hippocampus (Friedman and Goldman-Rakic 1988), entorhinal cortex (Suzuki et al. 1997), PRC (Davachi and Goldman-Rakic 2001) and PHC (Bachevalier and Nemanic 2008) contribute to the encoding and recall of information from short term memory. These animal findings complement neuropsychological studies of patients with amnesia resulting from Korsakoff's Syndrome, encephalitis and colloid cysts (Holdstock et al. 1995), and patients with surgical (Aggleton 1992; Owen et al. 1995) or ischemic (Holdstock et al. 2002) lesions to the MTL, demonstrating retention deficits for novel stimuli over delay intervals as short as two seconds (Ranganath and Blumenfeld 2005).

An increasing body of evidence further suggests that short term memory exploits the same MTL modules as episodic memory; that is, PRC codes information about an object's identity and PHC codes an object's location and its context, and these two streams are bound in the hippocampus (Pertzov et al. 2013; Watson et al. 2013; Yee et al. 2014; Libby et al. 2014). Consistent with the idea that in short term memory identity and location information are processed separately and then bound, patients with hippocampal damage can exhibit deficits recalling object-location conjunctions after 1.0s delays, even when unimpaired recalling either object identities or locations (Olson et al. 2006a; 2006b). However, other studies report that patients with damage to the hippocampus do not necessarily show deficits in recalling object-location conjunctions, suggesting that spatial binding is preserved (e.g. Jeneson et al. 2010; see Yonelinas 2013 for a review).

An alternative possibility is that spatial binding in short term memory occurs in parahippocampal regions, rather than the hippocampus proper. In support of this view, data in both rats (Burwell and Amaral 1998) and monkeys (Suzuki and Amaral 1994) indicate that PRC and PHC are reciprocally connected, suggesting that the parcellation of identity and spatial information is not absolute, and that there may already be substantial cross-talk between object and spatial/context related information in parahippocampal regions. Further, recordings in rats have demonstrated single unit responses for object-location conjunctions in the PHC homologue (Barker and Warburton 2011).

Behavioural studies in monkeys have provided crucial evidence for the role of PHC in spatial binding. Rhesus monkeys with PHC lesions are impaired in both simple location and object-location conjunction tasks (Malkova and Mishkin, 2003). This short term memory impairment was observed in a delayed match-to-sample task, where the sample contained two non-identical objects. After a six-second delay, the test array contained one of the objects in its original location (the target), and an identical item either at the location of the sample foil (object-place condition), or at a novel location not previously occupied by either sample object (location condition). Monkeys with PHC lesions were impaired identifying the target in both conditions, while monkeys with lesions in the hippocampus showed no impairment in either task (Malkova and Mishkin 2003). Hippocampectomised monkeys were likewise unimpaired in a later study, using a more difficult task with an increased number of objects and locations (Belcher et al. 2006).

A cross-species homology in the short term memory functionality of PHC is partly supported by the observation that patients with PHC lesions also exhibit a decrement in spatial recall (Ploner et al. 2000), although this impairment is only observed using delays greater (i.e. >15.0s) than those used by Malkova and Mishkin (2003). In addition, functional imaging data in healthy subjects demonstrate heightened right PHC activation during both encoding and maintenance of object-location conjunctions, relative to trials where objects or locations are memorised separately (Luck et al. 2010). However, no neuropsychological study has so far demonstrated that PHC contributes to spatial binding in human short term memory.

In the present study, we examined the nature and extent of spatial and short term memory deficits associated with focal PHC lesions, by testing a middle-aged man (PJ) with bilateral posterior circulation strokes involving the PHC, but sparing the hippocampus and PRC. Our experiments were driven by three specific research questions: 1) does damage to PHC produce binding difficulties and if so, are the binding problems specifically spatial or do they generalise to other visual dimensions; 2) do binding impairments reflect deficits in memory encoding or maintenance; and 3) is the binding impairment secondary to a loss of positional information either in memory or perception?

Both PJ and controls showed dependent decrements in the precision of spatial recall, however PJ's recall precision was significantly worse than controls at longer delays (5.0s). PJ also showed impaired spatial binding. This impairment was unaffected by the duration of the memory delay. Finally, PJ's binding deficits did not generalise across visual dimensions, since he performed normally when recall involved the conjunction of non-spatial features. We conclude that PHC serves a spatially specific binding function in short term memory, and that this function appears to be independent of PHC's role in recall precision.

Methods

PJ: history and clinical assessment

PJ was first seen by one of the authors (CR), four months after he had suffered a cerebrovascular accident. PJ was 45 years old when he developed headaches, visual and mental status changes over the course of a few hours. Two days after the onset of these symptoms, he was admitted to a stroke-unit at a regional hospital. During the admission, he continued to be confused and agitated. The diagnostic work-up revealed bilateral posterior circulation strokes involving the occipito-temporal cortex. No cause for the stroke was identified. PJ had no significant medical history, except for cluster headaches, which responded well to standard treatment.

Upon returning home, he was not able to resume his full-time occupation as an animal breeder, because of difficulties finding his way around the house and farm, where he had moved two years prior. He also relinquished driving, because he could not find his way around familiar streets. He was able to sketch the overall layout of his home, but frequently misidentified rooms and the family resorted to placing signs on internal doors to help him find his way around. His ability to repair equipment around the farm was also diminished, because of difficulty identifying the correct tool in a cluttered environment.

PJ's visual perimetry was formally assessed three and five months following the ischemic injury, with a binocular field test (Esterman, 1982). He showed strict upper quadrantanopias, worse on the left than on the right. There was evidence of partial recovery on the second assessment (see figure S3).

Formal clinical psychometric testing was conducted approximately 6 months following his stroke. The standardised scores are presented in table 1. His general intellectual functioning fell within the average range, as measured with the Wechsler Adult Intelligence scale, fourth edition (WAIS-IV). This was affected negatively by slowed processing speed on visual tasks. He performed similarly on the verbal (Verbal Comprehension Index) and non-verbal scale (Perceptual Reasoning Index) of the WAIS-IV. His expressive and receptive language functions were grossly intact. He did however often require verbal instructions to be repeated. His information-processing speed was in the borderline range on the WAIS-IV. Memory function was significantly impaired for both visual and verbal material. He had difficulties with learning and acquisition of new material and also with delayed recall. Performance was not improved for recognition memory. His errors on a visual memory task were primarily misplacement errors. He demonstrated set-loss errors on a word generation task and also required reminding of rules on a problem-solving task. Performance on executive functioning tasks was mixed; he performed at the expected level on a planning and problem-solving task. His performance on a verbal fluency task was within normal limits. His score on an attention-shifting and inhibition task was in the impaired range of ability. PJ passed on all subtests of object perception from the Visual Object and Space Perception Battery (Warrington and James 1991), except for progressive silhouettes, where he had a raw score of 11, indicating mild impairment. He was also faultless in all subtests of space perception.

PJ was scanned using a research MRI protocol and tested behaviourally at the Bangor University School of Psychology approximately one year and ten months following the ischemic event, when he was 47 years of age. Testing took place on two

consecutive days.

Control Participants

Behavioural comparison: Ten right-handed, healthy male participants were recruited from the local community. Controls were screened for any history of major neuropsychiatric disorders and visual impairments. IQ was measured with the 2-subtest (vocabulary and matrix reasoning) version of the Wechsler Abbreviated Scale of Intelligence (WASI; Wechsler 1999). Table 2 summarises the characteristics of the control group. The mean age was 48.2 years (sd: 6.4), the mean IQ was 101.1 (sd: 7.6) and the mean age leaving school was 16.6 (sd: 0.7). On all these variables, PJ and controls were matched; all p-values were above .095 using a modified t-test (Crawford and Howell 1998).

Anatomical comparison: A convenience sample of 10 healthy male participants was drawn from a Bangor University image register. The mean age was 43.3 years (sd: 4.9).

All participants were compensated for their time and travel expenses. All participants gave written, informed consent prior to initiating any experimental procedure. The testing procedures had been reviewed and approved by the Betsi Cadwaladr University Health Board and the Bangor University School Psychology Ethics committees.

Behavioural testing: overview and material

PJ and controls performed three computer-based behavioural experiments. Testing took place in a dark room; participants sat comfortably, unrestrained, approximately 85cm from an LCD screen (NEC LCD3210). Participants were encouraged to actively scan the display and foveate individual stimuli. Custom-coded Matlab scripts (Mathworks 2014a), using a set of freely available routines designed to facilitate the coding of visual experiments (Brainard 1997), controlled the experiments and generated the displays. Matlab scripts were run on an Apple iMac 10.

Statistical comparison of PJ and controls

We computed the significance of performance differences between PJ and the control group in all experiments using a modified t-test (Crawford and Howell 1998). Where performance was measured with a percentage or ratio, we conducted the t-test on logarithmically transformed values.

Imaging

Imaging – image acquisition and analysis

PJ and the anatomical comparison controls were scanned on a Phillips Achieva 3T MR scanner with a 32-channel head coil. T1 weighted images (TE = 4.32ms; 8° flip angle) were acquired axially with a 0.7mm isotropic voxel-size. PJ's T1 weighted anatomical volume was bias corrected and normalised to the atlas representative MNI152 template using SPM12 (Ashburner and Friston 2003). The mapping included a 12-degrees-of-freedom affine transform followed by a local deformation, computed after the lesion had been masked using a hand-drawn region. The normalised anatomy was obtained by interpolation via a 4th degree B-spline, and resampled using a 0.7mm linear voxel size. Skull stripped anatomy was obtained using a modified version of

FSL's BET, which is optimised for tissue segmentation in the presence of brain pathology (Lutkenhoff et al. 2014). To determine whether PJ's stroke encroached onto perirhinal and entorhinal cortex, probabilistic maps of these regions were superimposed on his brain anatomy (Hindy and Turk-Browne 2016). Lesion boundaries were drawn by a board-certified adult neurologist, using the co-registered T1 and FLAIR images.

Lesion anatomy results

Figure 1 shows axial and coronal slices from the MNI Atlas co-registered T1-weighted scan of PJ's brain. In the left hemisphere the lesion volume is 6.25 cm^3, in the right hemisphere 10.71 cm^3. Figure 1A shows that the ischemic lesions in medial occipitotemporal cortex (mOTC) of the left and right hemisphere lie posterior to the location of entorhinal and perirhinal cortex (marked respectively in red and green), identified in a previous group study (Hindy and Turk-Browne 2016). Figure S1 provides additional anatomical information about the relationship between lesion and entorhinal and perirhinal cortex. The coronal slices in figure 1B demonstrate that the fornix is intact, however sections -23 to -32 suggest hippocampal volume loss on the right. Also, retrosplenial cortex and the adjacent precuneus are spared in both hemispheres. Figure S2 shows sagittal slices through medial brain structures, which highlights the extent of the damage to PHC and lingual gyrus. Given the apparent hippocampal volume loss, we compared PJ's left and right hippocampal volumes to those of the anatomical comparison controls. A stereological procedure was used to estimate hippocampal volumes in all participants (Keller and Roberts 2009). The input images were the T1 weighted brain volumes in native scanner space. A regular cubic grid with a step of 3 pixels was superimposed on coronal slices, with a random

starting position. The senior author, a board-certified neurologist, outlined the hippocampal formation to determine the number of overlaying grid points. The hippocampal formation included the hippocampus, dentate gyrus and subiculum. The anterior border of the hippocampal formation was the alveus, the posterior border was the crux of the fornix. The hippocampal borders were also identified in axial and sagittal slices. The procedure was implemented using ImageJ (Schneider et al. 2012) and a stereology dedicated plugin (Merzin 2008). This analysis indicated that PJ's left (3931mm^3) and right (2530mm^3) hippocampi were not significantly smaller than controls (left: mean = 3561mm^3; $t(9) = 0.516$, $p = 0.618$; right: mean = 3816 mm^3 $t(9) = -1.79$, $p = 0.108$). However, the volumetric difference between the left and right hippocampi was significantly greater for PJ than for controls ($t(9) = 2.641$, $p = 0.027$), suggesting that PJ's right hippocampus may have been atrophied.

Experiment 1: spatial vs. non-spatial binding in working memory

Experiment 1 – Rationale

Primate studies (Malkova and Mishkin 2003; Belcher et al. 2006) have suggested that PHC is involved in remembering locations in close peri-personal space as well as spatial binding in working memory. In this first experiment, we examined visual working memory spatial and feature binding in PJ, a man with PHC lesions, and a group of age-matched controls. On each trial, participants had to remember the colour, shape and location of two objects. After a short delay, participants were cued to recall the colour of one of the objects, identified either by its location on the screen, or by its shape. We reasoned that if human PHC is involved in spatial binding, then PJ's recall performance should be worse than controls, specifically on location trials.

Experiment 1 – Methods

Figure 2A shows a schematic representation of Experiment 1's trial structure. In each trial, an equilateral triangle and a square, whose side lengths were 2.42° and 1.72° respectively, appeared side-to-side in the lower half of the screen, at an eccentricity of 4.25° along the main diagonal, for 2.0s. The shapes were either red, blue or green. A 200ms pattern mask, and then a 2.0s blank screen, followed the sample display. The recall screen contained three coloured rectangles, 1.0° wide and 3.0° high, whose lower edges were aligned 2.5° above the screen center and spaced horizontally 9.0° apart. A bright cross (location cue) or the outline of one of the two shapes (shape cue) identified the target. The location cues, which also included a dark cross, appeared at the locations occupied by the two shapes. The shape cue appeared 3.0° below the screen center. Participants reported the target colour by placing a cursor over the corresponding coloured rectangle and clicking the mouse button. The mouse click prompted the beginning of a new trial, after a 1.0s delay, during which the screen was blank. Participants practiced the task over ten trials and then completed ninety trials, including both shape and location cued recalls. Trial order was randomised, minimising participants' ability to predict whether a shape or location cue would follow the sample display. To ensure that PJ had not forgotten the task instructions, we asked him to describe what he had been doing after each block. In each instance he correctly reported that he had been recalling either the probed shape colour, or the colour at the location of the white cross.

Experiment 1 – Data analysis

We scored trials based on whether participants reported (a) the correct target colour (correct response), (b) the colour of the non-target shape (binding error), or (c) neither

the target nor the non-target colour, i.e., dummy colour (generic error). We then calculated the proportion of binding (BE) and generic errors (GE) for each cue condition ($_{location}$ and $_{shape}$) and compared PJ and the control group's recall accuracy using odds ratios. We computed two odds ratios: the first was the ratio of the proportion of binding errors in location vs. shape cued trials (i.e., [$BE_{location}$ / BE_{shape}]). The second was the ratio of binding errors over generic errors in location vs. shape cued trials (i.e., [$BE_{location}$ / $GE_{location}$] / [BE_{shape} / GE_{shape}]). If a participant's data cells contained zero counts, a value of 0.5 was added to all cells prior to computing the ratios (Gart and Zweifel 1967).

Experiment 1 – Results: impaired spatial binding in visual working memory

The left-hand panels of figures 2B and 2C report the proportion of generic errors following location and shape cues, while the right-hand panels show the proportion of binding errors. PJ made more binding errors when the target was identified by a location than a shape cue ($p < 0.001$; Fisher exact test). PJ was also much more likely to make a binding than a generic error following a location ($p< 0.001$, two-tailed binomial test), but not a shape cue ($p = 0.5$), suggesting that his difficulties did not reflect a problem remembering which colours had been shown. For PJ, the odds ratio of making a binding error in the location vs. shape cue trials was 60.7, which was significantly greater than the control group average of 0.501 (95% CI: [0.23 - 1.06], $t(9) = 3.72$, $p = 0.005$), suggesting that he was much more likely to make a binding error on location than shape cue trials, while controls were modestly more accurate following a location than a shape cue. Moreover, PJ's odds ratio of making a binding rather than a generic error in the location vs shape cued trials was 29.0 which was again significantly greater than the control group average of 0.421 (95% CI: [0.21 -

0.83], t(9) = 3.46, p = 0.007), confirming that he was much more likely to make a binding than a generic error on location rather than shape cued trials, while controls were more likely to make a binding than a generic error on shape rather than location trials.

Experiment 1: Interim discussion

PJ showed a remarkable deficit binding objects to their location in a working memory task. When he reported the colour of one of two objects, he was able to do so accurately for targets cued by their shape. However, when a target was identified by its location, his performance was greatly diminished because of numerous binding errors. Control participants, on the other hand, showed comparable recall accuracy irrespective of the cue type. These findings strongly suggest that PJ's impairment cannot be attributed to either diminished memory for the report feature, i.e. the target's colour, or a binding deficit that generalises across visual dimensions. Rather, PJ shows a binding impairment that is specifically spatial.

Experiment 2: delayed spatial recall

Experiment 2 – Rationale

In the previous experiment, we demonstrated that PJ suffers a specific spatial binding impairment in a working memory task. In experiment 2, we examined whether spatial binding impairments reflect diminished resolution of spatial data in working memory, or rather disruption of spatial binding. To this end we assessed the effects of the duration of the memory delay on both the precision of spatial recall and the proportion of binding errors.

Experiment 2 – Methods

Figure 3A summarises Experiment 2's trial structure. The sample stimulus consisted of three coloured discs, 0.8° in diameter. The discs were red, green and blue, and remained visible for 2.0s. A 1.0s long pattern mask followed the sample. A central colour cue (a 0.3° wide square) appeared either immediately after the pattern mask, or after an additional 4.0s interval, during which only a white central fixation point was visible. The cue identified the target of the same colour. The participants placed the cursor at the recalled target location and clicked the mouse to record their response and initiate the next trial. The location of the discs included the center of the screen and the vertices of a virtual square, at an eccentricity of 6.0°. 2D Gaussian displacement (s.d.= 0.9°) jittered the position of each disc. Each participant completed two blocks of one hundred and twenty trials each.

Experiment 2 – Data analysis

First, we identified trials in which participants had made a binding error, i.e. when the recalled position was closer to the one of the non-target items than the target, and the distance from the non-target item was no greater than half the minimum distance between canonical locations, i.e. 3.0° (Pertzov et al. 2013). After tabulating and removing binding errors, we estimated recall accuracy and precision. Accuracy reflects how close a participant's average reported location is to the true target position. Precision reflects the magnitude of trial-to-trial deviations from a participant's average reported location. Accuracy is diminished by systematic errors, which depend on factors such as display size and memory load (Katshu and d'Avossa 2014), while precision is thought to reflect the resolution of spatial memory (Bays et al. 2009). These two variables were computed using linear regressions. We computed

two regressions whose dependent variables were the azimuth and elevation of the reported target location, respectively. The regressors in each case included a constant and the target's azimuth and elevation. The results of the regression analysis were used to estimate the systematic biases reporting the target location. The scaling factor was the divergence of the error field, which we previously found to be the main linear component of the systematic error (Katshu and d'Avossa 2014). We quantified recall precision using the standard deviation of the residuals from the model fits. The variance and standard deviations of the variable errors were computed using the same procedure employed in a previous study (Katshu and d'Avossa 2014), and averaged over azimuth and elevation. Precision changes between short and long delays were quantified using an efficiency measure, namely a ratio whose numerator was the recall variance following 1.0s delays and denominator was recall variance following 5.0s delays.

Experiment 2 – Results: recall precision, but not binding errors, affected by memory delay

PJ made more binding errors than controls, following both 1.0s and 5.0s delays. Otherwise, both PJ and controls performed similarly in terms of accuracy and precision.

The proportion of binding errors are shown in the left-hand panels of figure 3B and 3C. Overall, PJ made a binding error on 9.44% of trials, which was significantly greater than the control group average of 3.21% (95% CI: [2.24 - 4.18]; $t(9) = 4.02$; $p = 0.003$). Increasing the duration of the memory delay had no effect on the proportion of PJ's relative binding errors; PJ's odds ratio for making a binding error following

1.0s vs. 5.0s delays was 1.27, which was not significantly different to the control group average of 1.0 (95% CI: [0.72 - 1.38]; t(9) = 0.462; p = 0.655), and suggested a non-significant tendency for more binding errors following short than long memory delays. Further, 40% (6/15) of PJ's binding errors on short delay trials, and 50% (6/12) of his binding errors on long delay trials, occurred when the target appeared in the upper portion of the screen; a goodness of fit test reported that his binding errors were not biased toward the target appearing in either the upper or lower half of the screen following either delay (χ^2 (3) = 1, p = .801). We can therefore conclude that his binding issues are unlikely due to his upper visual field deficit impacting the encoding of the entire sample stimulus.

Both PJ and controls showed systematic distortions. Following both short and long memory delays, PJ reported targets displaced leftward (1.0s: -0.24°; 5.0s: -0.23°) and upward (1.0s: 0.15°; 5.0s: 0.09°). In contrast, controls' group mean displacement was rightward (1.0s: 0.09°, 95% CI: [-0.09 – 0.26]; 5.0s: 0.07°, 95% CI: [-0.12 – 0.27];) and downward (1.0s: -0.37°, 95% CI: [-0.55 – -0.19]; 5.0s: -0.28°, 95% CI: [-0.45 – -0.11]). However, PJ's displacements were not significantly different from controls for both delays (all p-values > 0.100). PJ also tended to overestimate the position of targets relative to the screen center, indicated by an error divergence of 0.04 following 1.0s delays and 0.16 following 5.0s delays. In contrast, controls underestimated targets relative to the screen center, as indicated by a group average error divergence of -0.26 (95% CI: [-0.36 – -0.15]) following 1.0s delays and -0.29 (95% CI: [-0.41 – -0.16]) following 5.0s delays. However, PJ and controls did not differ significantly (both p-values > 0.055).

Recall precision data are summarised in the right-hand panel of figure 3B and 3C. In contrast to binding errors, increasing the delay had a significant effect on recall precision. PJ's error standard deviation was 1.33° following 1.0s delays, which was not statistically different from the control group average of 1.01° (95% CI: [0.91 – 1.10]; t(9) = 2.11; p = 0.064). PJ's error standard deviation following 5.0s delays (1.78°) was statistically larger than the control group average of 1.18° (95% CI: [1.09 – 1.27]; t(9) = 4.23; p = 0.002). However, PJ's efficiency after a 5.0s delay compared to a 1.0s delay was 0.56, which was not significantly smaller than the control group average of 0.73 (95% CI: [0.65 – 0.82]; t(9) = -1.37; p = 0.203).

Experiment 2: Interim discussion

The experiment yielded a number of findings. First PJ made more binding errors than controls, confirming that he exhibited an impairment of spatial binding using a task in which the target location was the report rather than the cue variable. Secondly, following 1.0s delay the precision recalling the target location was not appreciably different between PJ and controls, suggesting that his binding impairment did not reflect a problem recalling the target location precisely. Moreover, while increasing the memory delay did not increase the proportion of binding errors, it did significantly diminish both PJ and controls' spatial recall precision, providing additional evidence that recall precision did not account for binding errors. In summary, PJ shows frequent binding errors, but spatial recall precision which is comparable to that of controls. Crucially, changing the duration of the memory delay produces dissociable effects on recall precision and binding.

Experiment 3: centroid estimation

Experiment 3 – Rationale

In experiment 3 we ascertained whether PJ's diminished recall of a target position may reflect a sensory impairment. While this seems unlikely given the finding that PJ's recall precision was not significantly diminished compared to controls (with 1.0s delay), it was important to establish the extent to which sensory difficulties may have limited his performance. We therefore assessed participants' spatial accuracy and precision in a perceptual task.

Experiment 3 – Methods

This experiment assessed participants' ability to localise the centroid, namely the average location, of three white discs. The discs' diameter was 0.5° (see figure 4A for a schematic representation of the trial structure). The discs remained visible until participants had positioned a crosshair shaped cursor at the desired location and clicked the mouse. Following a blank, 1.0s-long interval, a novel set of discs appeared and the procedure was repeated. Discs could occupy any of seven canonical locations. These included the screen center and the vertices of a virtual concentric hexagon, with a side length of 6.87°. All permutations of three out of seven canonical target locations, less any resulting in a collinear configuration, were used as sample arrays. Each possible permutation appeared twice, for a total of sixty-four trials. A pseudorandom, zero mean, circular Gaussian distribution, with a standard deviation of 0.6°, was used to jitter each disc's position independently. Prior to testing, instructions were read to the participants. The centroid was defined as the point in space where the triangle, whose vertices coincided with the discs' locations, would balance in the horizontal plane (Baud-Bovy and Soechting 2001). One of the experimenters also provided a visual demonstration, using a cut-out triangular shape.

Prior to testing, participants completed twenty-five practice trials. At the end of each practice trial, the reported and actual positions of the centroid were shown for 2.0s.

Experiment 3 – Data analysis

We estimated the systematic and variable error of participants' centroid estimations, by fitting a linear model to the azimuth and elevation of the reported centroid location. The model regressors included a constant and the centroid azimuth and elevation. Two metrics were used to characterise the systematic error: 1) the constant displacement, that is the tendency to report the centroid above, below, right or left of its true location, and 2) scaling factor, measuring the linear relationship between reported and actual centroid positions. These are, respectively, the estimated intercept and beta parameters of the linear model. We computed precision as the standard deviation of the variable error, i.e., residuals from the model, using the same methods used in Experiment 2.

Experiment 3 – Results: accuracy and precision of centroid estimation

The left-hand panels of figure 4B and 4C illustrate the direction of systematic biases in centroid estimates. PJ and controls respectively reported the centroid -0.07° and -0.10° (95% CI: [-0.15° – -0.04°]) left of its veridical position, suggesting that both showed a similarly small leftward bias, ($t(9) = 0.322$, $p = 0.755$). However, PJ reported the centroid 0.56° above its veridical position. This bias was significantly larger than controls, who showed a group average upward bias of 0.06° (95% CI: [-0.02° – 0.14°]; $t(9) = 3.69$, $p = 0.005$). The middle panel of figure 4B and 4C summarise the linear scaling for centroid estimates. PJ varied the reported centroid azimuth by a factor of 0.97, and elevation by a factor of 1.00, in both cases reflecting

an almost perfect linear relationship between reported an actual centroid positions. These values were comparable to those shown by controls, namely 0.99 for azimuth (95% CI: [0.94 – 1.03]; t(9) = -0.263, p = 0.799), and 0.97 for elevation (95%CI: [0.93 – 1.01]; t(9) = 0.443, p = 0.668). Finally, PJ's azimuth variable error standard deviation, 0.67°, was not significantly different from the control average of 0.69° (95%CI = [0.56° - 0.82°]; t(9) = -0.091, p = 0.931), nor was his elevation variable error standard deviation, 0.77°, significantly different from the control average of 0.59° (95%CI = [0.47° - 0.70°]; t(9) = 0.925, p = 0.380), suggesting that both the vertical and horizontal precision of his centroid judgements was relatively spared.

Experiment 3 – Interim discussion

PJ showed a strong tendency to report the centroid above its true location. This probably represents a compensatory strategy for his upper visual field defect. In fact, hemianopic patients display a bias toward their blind field when judging the midpoint of horizontal line (Barton and Black 1998; Kerkhoff and Buchers 2008). However, both PJs accuracy and precision estimating the centroid position were within the control group's range. We conclude that aside from compensatory visual defect biases, PJ's ability to localise perceptually is largely spared and unlikely to account for his diminished recall precision.

Discussion

We tested a middle-aged man (PJ) with bilateral mOTC strokes involving the PHC. Acutely, PJ had developed a derangement of attention and short-term memory (Horenstein et al. 1967; Medina et al. 1977; Shih et al. 2007). At the time of testing, PJ was no longer delirious, but continued to have difficulties with his memory as well as navigating familiar environments. The latter is a form of spatial disorientation previously attributed to PHC lesions in humans (Zola-Morgan et al. 1989; Epstein et al. 2001). Animal studies have demonstrated additional deficits in spatial working memory following PHC lesions in non-human primates (Malkova and Mishkin 2003; Bachevalier and Nemanic 2008). Whether the same deficits characterise human patients with PHC lesions is not yet known.

We found that PJ had a profound deficit binding an object to its location in a working memory task. When he recalled the colour of one of two objects, after a short memory delay, he could accurately do so when the target was cued by its shape. However, when the target was cued by its location, his accuracy was greatly diminished because he made numerous binding errors, frequently reporting the colour of the non-target item instead of the colour of the target. Control participants, on the other hand, were accurate whether the target was identified by the location or shape cue. These findings strongly suggest that PJ was impaired only when using a location cue and that this impairment could not be attributed to either diminished memory for the report feature, i.e. the target's colour, or a binding deficit that generalises across spatial and non-spatial visual dimensions. According to a recent study, generalised binding difficulties may instead characterise recall performance in individuals with autoimmune temporal encephalitis, which mainly affects the hippocampal formation (Pertzov et al. 2013).

Some animal and imaging studies have indeed shown that both anterior PHC and hippocampus contribute to object-in-place associations in short-term memory (Milner et al. 1997; Bachevalier and Nemanic 2008). However, animal data suggest that hippocampal involvement in spatial binding is restricted to tasks where spatial relations are incidentally encoded (Bachevalier and Nemanic 2008). These findings, together with ours, suggest that in tasks where spatial information is intentionally encoded and recalled, the role of PHC goes beyond simply providing spatial data to the hippocampus, where general purpose processes bind visual features in working memory. Moreover, our findings confirm that binding in visual working memory is liable to be disrupted by focal brain lesions (Gorgoraptis et al. 2011), supporting the idea that it is a neural function independent from those underpinning the representations of individual features (Wheeler and Treisman 2002; Smyrnis et al. 2005).

Binding errors do not reflect the resolution of spatial information

When PJ reported the location of one of three objects held in memory he erroneously reported the location of one of the non-target items more frequently than controls. This finding suggests that PJ had difficulties with spatial binding, whether space was the cue or report dimension. One might argue that PJ's spatial binding impairment simply reflects degraded spatial representations. In other words, diminished ability recalling the location of an object might explain his difficulties using spatial information to identify targets in memory. However, this hypothesis is not supported by our data. PJ was able to estimate the centroid of simple dot configurations as precisely as controls, indicating that despite the presence of an upper visual field

defect, the spatial resolution of visual data was not prominently affected in this perceptual task. Moreover, PJ's precision recalling the location of visual targets was not appreciably different from that of controls, even though his proportion of spatial binding errors was much greater. Finally, binding errors did not become more frequent when the delay interval was increased, although the precision of spatial recall did decrease. We conclude that binding errors do not reflect the temporal decay of a memory trace, contrary to previous suggestions (Zhang and Luck 2009). Moreover, our findings are consistent with observations that binding errors are not affected by the duration of the memory delay in either patients with hippocampal pathology (Pertzov et al. 2013) or healthy controls (Gorgoraptis et al. 2011), although whether binding errors may be effected by longer (e.g., >20.0s) delays remains to be established. Finally, varying the spatial memory demands at the time of recall in a spatial version of the Sternberg working memory task does not change the likelihood of committing a binding error, confirming that binding errors do not reflect confusion among features of the probe dimension (Smyrnis et al. 2005). Taken together, the available evidence in healthy controls and patients instead suggests that binding errors reflect interference with early processes, engaged at the time when visual information is encoded in working memory. However, a recent high-resolution fMRI study has suggested that load dependent signals in PHC during the delay period of a match-to-sample-task may reflect on-going binding processes (Schon et al. 2016).

Delays affect the precision of spatial recall

PJ's spatial recall precision was similar to that of controls when the memory delay lasted 1.0s. When the memory delay was 5.0s long, both he and controls suffered a decrement in recall precision. These are not entirely novel findings. Recall precision

is known to decrease with longer memory delays in healthy controls (Sheth and Shimojo 2001; Zhang and Luck 2009). Moreover, recall precision disproportionally decreases in patients with PHC lesions, although significantly so only following memory delays greater than 20s (Ploner et al. 2000). This finding is in keeping with our own: recall efficiency following 5.0s vs 1.0s delays was lower in PJ than in controls, however this difference was not significant. Combined, these data are consistent with the idea that following PHC lesions, spatial recall precision decays more quickly than in healthy controls, as opposed to declining abruptly. More generally, our findings are in keeping with the view that spatial recall draws information from a limited capacity resource (Bays et al. 2009), whose resolution diminishes over time. Therefore, delay dependent changes in spatial recall precision most likely reflect a limited ability to maintain information in working memory rather than impaired encoding, in contrast to the binding deficits discussed above. Finally, PJ's performance in our experiments is consistent with his neuropsychological profile, which is principally characterised by impairment on various memory tasks, including those that do not have a spatial binding component, such as the Logical Memory test and the Rey Auditory Verbal Learning Test. However we do not yet know the extent to which diminished recall precision and spatial binding account for the broad memory deficits observed following lesions to PHC.

Could the hippocampus be the site for short term memory spatial binding?

In the present study we identified impairments resulting from focal lesions to PHC, and found a spatial binding deficit in short term memory. Our data cannot rule out the possibility that binding takes place outside PHC, for example, in the hippocampus. Indeed, comparison of hippocampal volumes in PJ and age and gender matched

controls suggest hippocampal atrophy in PJ. Lateralised hippocampal atrophy commonly follows distal, ipsilateral stroke, even in young patients unlikely to harbour neurodegenerative processes (Schaapsmeerders et al. 2015a, 2015b), suggesting that the hippocampus may be particularly vulnerable to the effects of deafferentation. Pj's hippocampal atrophy raises the possibility that spatial binding deficits reflect diminished function within the hippocampus. Our data cannot refute this alternative hypothesis. As mentioned in the introduction, previous studies in patients with inflammatory and anoxic damage involving the hippocampus (e.g. Pertzov et al. 2013; Watson et al. 2013; Yee et al. 2014) have also demonstrated spatial binding impairments, lending support to the hippocampus' role in feature binding. Nonetheless, the specific spatial nature of PJ's binding impairment, which did not generalise to other visual dimensions (i.e., shape), is inconsistent with the proposal that the hippocampus provides a general purpose binding mechanism. Therefore, we conclude that spatial binding is either carried out in hippocampus, using inputs from PHC, or that PHC itself initiates spatial binding processes.

Concluding remarks

This study provides novel information on the role of MTL, by showing that a man with a lesion involving PHC, hippocampal atrophy, but spared PRC, has a selective deficit in short term spatial binding. This deficit is not explained by diminished resolution of spatial information. Our findings are consistent with the idea that spatial binding processes in short term memory may be initiated in the PHC even before visual information reaches the hippocampus.

Acknowledgments

This work was supported in part by the Biotechnology and Biological Sciences Research Council grant BB/1007091/1. The authors thank Paul Mullins for his assistance with MRI data acquisition, and for providing the anatomical control data.

References

Aggleton JP. 1992. The functional effects of amygdala lesions in humans: A comparison with findings from monkeys. New York (NY): Wiley-Liss.

Ashburner J, Friston KJ. 2003. Spatial normalization using basis functions. In: Frackowiak RS, Friston KJ, Frith CD, Dolan RJ, Price CJ, Ashburner J, Penny WD, Zeki S, editors. Human brain function. Oxford: Academic Press. p. 655-672.

Bachevalier J, Nemanic S. 2008. Memory for spatial location and object-place associations are differently processed by the hippocampal formation, parahippocampal areas TH/TF and perirhinal cortex. Hippocampus. 18(1):64-80.

Barker GR, Warburton EC. 2011. When is the hippocampus involved in recognition memory? J Neurosci. 31(29):10721-10731.

Barton JJ, Black SE. 1998. Line bisection in hemianopia. J Neurol Neurosurg Psychiatry. 64(5):660-662.

Baud-Bovy G, Soechting J. 2001. Visual localization of the center of mass of compact, asymmetric, two-dimensional shapes. J Exp Psychol Hum Percept Perform. 27(3):692-706.

Bays PM, Catalao RF, Husain M. 2009. The precision of visual working memory is

set by allocation of a shared resource. J Vision. 9(10):7-7.

Belcher AM, Harrington, RA, Malkova, L, Mishkin, M. 2006. Effects of hippocampal lesions on the monkey's ability to learn large sets of object-place associations. Hippocampus. 16(4):361-367.

Brainard DH. 1997. The psychophysics toolbox. Spatial vision. 10:433-436.

Burwell RD, Amaral DG. 1998. Perirhinal and postrhinal cortices of the rat: interconnectivity and connections with the entorhinal cortex. J Comp Neurol. 391(3):293-321.

Corkin S. 1984, June. Lasting consequences of bilateral medial temporal lobectomy: Clinical course and experimental findings in HM. Semin Neurol. 4(2):249-259.

Corkin S, Amaral DG, González RG, Johnson KA, Hyman, BT. 1997. HM's medial temporal lobe lesion: findings from magnetic resonance imaging. J Neurosci. 17(10):3964-3979.

Crawford JR, Howell DC. 1998. Comparing an individual's test score against norms derived from small samples. Clin Neuropsychol. 12(4):482-486.

Davachi L, Goldman-Rakic PS. 2001. Primate rhinal cortex participates in both visual recognition and working memory tasks: functional mapping with 2-DG. J Neurophys. 85(6):2590-2601.

Deacon RM, Bannerman DM, Kirby BP, Croucher A, Rawlins JNP. 2002. Effects of cytotoxic hippocampal lesions in mice on a cognitive test battery. Behav Brain Res. 133(1):57-68.

Diana RA, Yonelinas AP, Ranganath C. 2007. Imaging recollection and familiarity in the medial temporal lobe: a three-component model. Trends Cogn Sci. 11(9):379-386.

Eichenbaum H, Yonelinas AR, Ranganath C. 2007. The medial temporal lobe and recognition memory. Annu Rev Neurosci. 30:123.

Epstein R, DeYoe EA, Press DZ, Rosen AC, Kanwisher N. 2001. Neuropsychological evidence for a topographical learning mechanism in parahippocampal cortex. Cognitive Neuropsychol. 18(6):481-508.

Esterman B. (1982). Functional scoring of the binocular field. Ophthalmology. 89:1226-1234.

Friedman HR, Goldman-Rakic PS. 1988. Activation of the hippocampus and dentate gyrus by working-memory: a 2-deoxyglucose study of behaving rhesus monkeys. J Neurosci. 8(12):4693-4706.

Gorgoraptis N, Catalao RF, Bays PM, Husain M. 2011. Dynamic updating of working memory resources for visual objects. J Neurosci. 31(23):8502-8511.

Graham KS, Barense MD, Lee AC. 2010. Going beyond LTM in the MTL: a synthesis of neuropsychological and neuroimaging findings on the role of the medial temporal lobe in memory and perception. Neuropsychologia. 48(4):831-853.

Habib M, Sirigu A. 1987. Pure topographical disorientation: a definition and anatomical basis. Cortex. 23(1):73-85.

Hindy NC, Turk-Browne NB. 2016. Action-based learning of multistate objects in the medial temporal lobe. Cereb Cortex. 26(5):1853-1865.

Holdstock JS, Shaw C, Aggleton JP. 1995. The performance of amnesic subjects on tests of delayed matching-to-sample and delayed matching-to-position. Neuropsychologia. 33(12):1583-1596.

Holdstock JS, Mayes AR, Roberts N, Cezayirli E, Isaac CL, O'Reilly RC, Norman KA. 2002. Under what conditions is recognition spared relative to recall after selective hippocampal damage in humans?. Hippocampus. 12(3):341-351.

Horenstein S, Chamberlin W, Conomy J. 1967. Infarction of the fusiform and calcarine regions: agitated delirium and hemianopia. T Am Neurol Assoc. 92:85.

Jeneson A, Mauldin KN, Squire LR. 2010. Intact working memory for relational

information after medial temporal lobe damage. J Neurosci. 30(41):13624-13629.

Katshu MZUH, d'Avossa G. 2014. Fine-grained, local maps and coarse, global representations support human spatial working memory. PloS one. 9(9):e107969.

Keller SS, Roberts N. 2009. Measurement of brain volume using MRI: software, techniques, choices and prerequisites. J Anthropol Sci. 87:127-51.

Kerkhoff G, Bucher L. 2008. Line bisection as an early method to assess homonymous hemianopia. Cortex. 44(2):200-205.

Libby LA, Hannula DE, Ranganath C. 2014. Medial temporal lobe coding of item and spatial information during relational binding in working memory. J Neurosci. 34(43):14233-14242.

Luck D, Danion JM, Marrer C, Pham BT, Gounot D, Foucher J. 2010. The right parahippocampal gyrus contributes to the formation and maintenance of bound information in working memory. Brain Cognition. 72(2):255-263.

Lutkenhoff ES, Rosenberg M, Chiang J, Zhang K, Pickard JD, Owen AM, Monti MM. 2014. Optimized brain extraction for pathological brains (optiBET). PLoS One. 9(12):e115551.

Malkova L. Mishkin M. 2003. One-trial memory for object-place associations after separate lesions of hippocampus and posterior parahippocampal region in the monkey. J Neurosci. 23(5):1956-1965.

Medina JL, Chokroverty S, Rubino FA. 1977. Syndrome of agitated delirium and visual impairment: a manifestation of medial temporo-occipital infarction. J Neurol Neurosurg Psychiatry. 40(9):861-864.

Merzin M. 2008. Applying stereological method in radiology. Volume measurement. Bachelor's thesis. University of Tartu.

Olson IR, Page K, Moore KS, Chatterjee A, Verfaellie M. 2006a. Working memory for conjunctions relies on the medial temporal lobe. J Neurosci. 26(17):4596-4601.

Olson IR, Moore KS, Stark M, Chatterjee A. 2006b. Visual working memory is impaired when the medial temporal lobe is damaged. J Cog Neurosci. 18(7):1087-1097.

Owen AM, Sahakian BJ, Semple J, Polkey CE, Robbins TW. 1995. Visuo-spatial short-term recognition memory and learning after temporal lobe excisions, frontal lobe excisions or amygdalo-hippocampectomy in man. Neuropsychologia. 33(1):1-24.

Pertzov Y, Miller TD, Gorgoraptis N, Caine D, Schott JM, Butler C, Husain M. 2013.

Binding deficits in memory following medial temporal lobe damage in patients with voltage-gated potassium channel complex antibody-associated limbic encephalitis. Brain. awt129.

Ploner CJ, Gaymard BM, Rivaud-Péchoux S, Baulac M, Clémenceau S, Samson S, Pierrot-Deseilligny C. 2000. Lesions affecting the parahippocampal cortex yield spatial memory deficits in humans. Cereb Cortex. 10(12):1211-1216.

Ranganath C, Blumenfeld RS. 2005. Doubts about double dissociations between short-and long-term memory. Trends Cogn Sci. 9(8):374-380.

Reisel D, Bannerman DM, Schmitt WB, Deacon RM, Flint J, Borchardt T, Seeburg PH, Rawlins JNP. 2002. Spatial memory dissociations in mice lacking GluR1. Nat Neurosci. 5(9):868-873.

Schaapsmeerders P, van Uden IW, Tuladhar AM, Maaijwee NA, van Dijk EJ, Rutten-Jacobs LC, Arntz RM, Schoonderwaldt HC, Dorresteijn LD, de Leeuw FE, Kessels RP. 2015. Ipsilateral hippocampal atrophy is associated with long‐term memory dysfunction after ischemic stroke in young adults. Hum Brain Mapp. 36(7):2432-2442.

Schaapsmeerders P, Tuladhar AM, Maaijwee NA, Rutten-Jacobs LC, Arntz RM, Schoonderwaldt HC, Dorresteijn LD, van Dijk EJ, Kessels RP, de Leeuw FE. 2015. Lower ipsilateral hippocampal integrity after ischemic stroke in young adults: a long-term follow-up study. PloS One. 10(10):p.e0139772.

Schneider CA, Rasband WS, Eliceiri KW. 2012. NIH Image to ImageJ: 25 years of image analysis. Nat Methods. 9:671-675.

Schon K, Newmark RE, Ross RS, Stern CE. 2016. A working memory buffer in parahippocampal regions: evidence from a load effect during the delay period. Cereb Cortex. 2016. 26(5):1965-74.

Scoville WB, Milner B. 1957. Loss of recent memory after bilateral hippocampal lesions. J Neurol Neurosurg Psychiatry. 20(1):11-21.

Sheth BR, Shimojo S. 2001. Compression of space in visual memory. Vision Res. 41(3):329-341.

Shih H, Huang W, Liu C, Tsai T, Lu C, Lu M, Chen P, Tseng C, Jou S, Tsai C, Lee CC. 2007. Confusion or delirium in patients with posterior cerebral arterial infarction. Acta Neurol Taiwanica. 16(3):136-142.

Smyrnis N, d'Avossa G, Theleritis C, Mantas A, Ozcan A, Evdokimidis I. 2005. Parallel processing of spatial and serial order information before moving to a remembered target. J Neurophysiol. 93(6):3703-3708.

Suzuki WA, Miller EK, Desimone R. 1997. Object and place memory in the macaque entorhinal cortex. J Neurophysiol. 78(2):1062-1081.

Suzuki WL, Amaral DG. 1994. Perirhinal and parahippocampal cortices of the macaque monkey: cortical afferents. J Comp Neurol. 350(4):497-533.

Warrington EK, James M. 1991. The visual object and space perception battery. Bury St Edmunds (United Kingdom): Thames Valley Test Company.

Watson PD, Voss JL, Warren DE, Tranel D, Cohen NJ. 2013. Spatial reconstruction by patients with hippocampal damage is dominated by relational memory errors. Hippocampus. 23(7):570-580.

Wechsler D. 1999. Wechsler abbreviated scale of intelligence. Psychological Corporation.

Wheeler ME, Treisman AM. 2002. Binding in short-term visual memory. J Exp Psychol Gen. 131(1):48-64.

Yee LT, Hannula DE, Tranel D, Cohen NJ. 2014. Short-term retention of relational memory in amnesia revisited: accurate performance depends on hippocampal integrity. Front Human Neurosci. 8(16).

Yonelinas AP. 2013. The hippocampus supports high-resolution binding in the service of perception, working memory and long-term memory. Behav Brain Res. 254:34-44.

Zhang W, Luck SJ. 2009. Sudden death and gradual decay in visual working memory.

Psychol Sci. 20(4):423-428.

Zola-Morgan S, Squire LR, Amaral DG, Suzuki WA. 1989. Lesions of perirhinal and parahippocampal cortex that spare the amygdala and hippocampal formation produce severe memory impairment. J Neurosci. 9(12):4355-4370.

Tables

Neurocognitive domain / Test / Subtest	Raw score	Standard/Z Score	Percentile
Intellectual Functioning			
Wechsler Intelligence Scale - IV			
Full Scale IQ		87	19
Verbal Comprehension Index		96	39
Perceptual Reasoning Index		90	25
Working Memory Index		92	25
Processing Speed Index		79	8
Vocabulary		9	37
Similarities		9	37
Information		10	50
Block Design		9	37
Matrix Reasoning		5	5
Visual Puzzles		11	63
Digit Span		9	37
Arithmetic		8	25
Symbol Search		7	16
Coding		5	5
Learning and Memory			
Wechsler Memory Scale			
Logical Memory I	11/75	2	0.4
Logical Memory II	4/50	3	1
Visual Reproduction I	56	4	2

Visual Reproduction II	13	5	5
Auditory Verbal Learning Test			
Trial I	3	-2	2
Trial II	4	-2.33	1
Trial III	5	-2	2
Trial IV	8	-1.15	13
Trial V	5	-3.31	1
List B	4	-1.11	13
Trial VI	3	-2.2	2
Delayed Recall	1	-2.54	1
Recognition	1	-4.3	1
Rey Complex Figure Test			
Copy	36	1.38	92
30 minute recall	1.5	-2.25	< 1
Benton Visual Retention Test			
Correct score	3	-2.69	< 1
Error score	13	-3.35	< 1
Attention/Executive Function			
Trail Making Test			
Part A	72 sec	-4.05	< 1
Part B	131 sec	-4.66	< 1
D-K Executive Function System			
Verbal Fluency Test			

Letter Fluency	25	6	9
Category Fluency	39	10	50
Tower Test			
Total Achievement Score	16	10	50
Stroop Test			
Colour task	112		
Colour-word task	38		> 2

Object recognition and Space Perception

The Visual Object and Space Perception Battery	
Object Perception	
Screening Test	20/20 (Pass)
Incomplete Letters	19/20 (Pass)
Silhouettes	19/30 (Pass)
Object Decision	17/20 (Pass)
Progressive Silhouettes	11 (Fail)
Space Perception	
Dot Counting	10/10 (Pass)
Position Discrimination	20/20 (Pass)
Number Location	10/10 (Pass)
Cube Analysis	10/10 (Pass)

Table 1. Summary of PJ's neuropsychometric performance six months after stroke.

Gender	Handed	Age	IQ	Age Leaving School
M	Right	51	106	18
M	Right	43	111	16
M	Right	45	99	16
M	Right	61	103	17
M	Right	39	109	18
M	Right	47	90	16
M	Right	53	88	16
M	Right	46	104	17
M	Right	53	97	16
M	Right	44	104	16
	Mean	48.2	101.1	16.6
	SD	6.4	7.6	0.8

Table 2. Control group demographics and IQ

Captions

Figure 1. Lesion anatomy. T1 weighted, MNI atlas registered axial (panel A) and coronal (panel B) slices are displayed in neurological coordinates, and illustrate the extent of ischemic damage in the left and right mOTC. In panel A, the axial slices also highlight the location of entorhinal and perirhinal cortex, in red and green respectively. These regions lay anteriorly and laterally to the boundaries of the ischemic lesions. In panel B, coronal slices highlight parahippocampal and hippocampal structures, including the fornix. The ischemic lesions lay inferiorly and posteriorly to the hippocampus and spare the fornix and the retrosplenial cingulate cortex.

Figure 2. Spatial vs. non-spatial binding in working memory. Panel A shows the trial structure. The sample display for all participants (including PJ) contained a square and a triangle, placed side by side in the bottom half of the screen. The two objects were red, blue or green and never had the same colour. After a brief pattern mask and blank delay, three vertical coloured bars appeared as well as a cursor, which the participant used to report the colour of the memory target. In shape trials, targets were identified by a probe whose outline matched the target shape. In location trials, the location of targets were identified by a white cross. Panel B shows each individual participants' error rate on a greyscale, with lighter colours representing a higher proportion of errors; the left panel shows generic errors, the right panel shows binding errors. On each panel, the upper row shows errors following shape probes, while the lower row shows errors following location probes, for PJ (blue outline) and each of the controls (red outline). Panel C shows PJ's and the group averaged proportion of generic and binding errors. Error bars are standard error of the mean.

Figure 3. Delayed spatial recall. Panel A shows the structure of immediate and delayed, spatial recall trials. The sample display for all participants (including PJ) contained three coloured discs, which could appear in both the upper and lower portion of the screen. The participants had to reproduce the position of one of the discs (the target) using a mouse cursor after either a 1.0s pattern mask or an additional 4.0s delay. The target was identified by its colour, indicated by a visual probe displayed at the center of the screen. Panel B (left) shows PJ's (blue outline) and controls' (red outline) individual percentage of binding errors on a greyscale, following 1.0s (upper row) and 5.0s (lower row) delays, with lighter colours representing a higher proportion of errors. Panel B (right) shows recall precision (95% error ellipses) in 1.0s and 5.0s delayed recall trials for PJ (blue) and controls (red). Panel C shows PJ's and the group averaged proportion of binding errors and precision. Error bars are standard error of the mean.

Figure 4. Centroid estimation. Panel A shows the trial structure. The participants placed a cursor at the centroid of the configuration formed by three bright discs. The discs remained visible until the participant made a response by clicking the mouse. Panel B shows each participant's constant displacement (arrow vectors), scaling (diamond plot) and precision (uncertainty ellipses) in locating the centroid. The length of the diamond plot's hemi-axes corresponds to 1.0 scaling factor. Panel C shows PJ's and group averaged values of the constant displacement and scaling factor, separately for azimuth (X) and elevation (Y). The precision measure shown is the square root of the mean error variance for azimuth and elevation. Error bars in all cases are standard error of the mean.

976

977

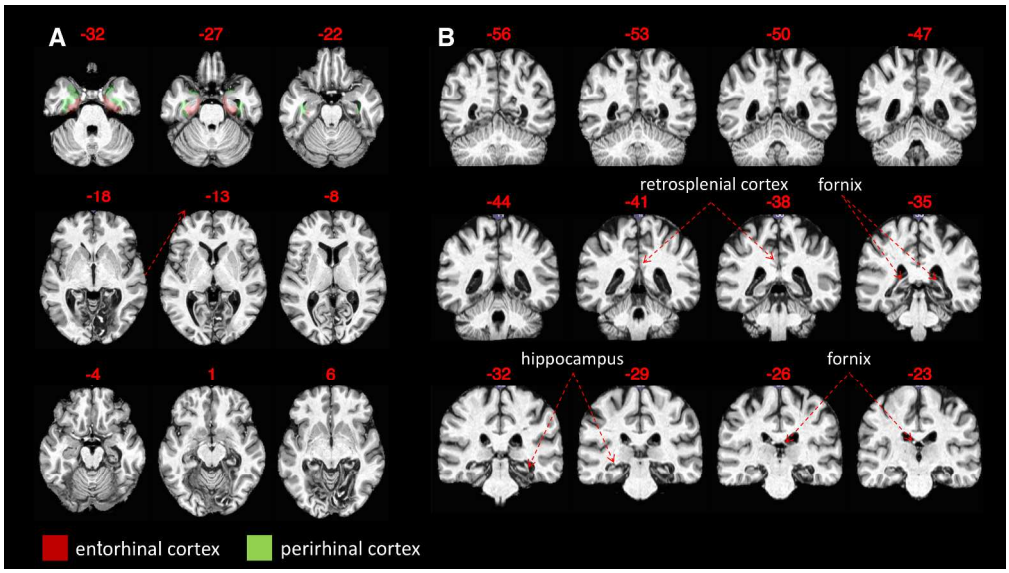

Figure 1. Lesion anatomy. T1 weighted, MNI atlas registered axial (panel A) and coronal (panel B) slices are displayed in neurological coordinates, and illustrate the extent of ischemic damage in the left and right mOTC. In panel A, the axial slices also highlight the location of entorhinal and perirhinal cortex, in red and green respectively. These regions lay anteriorly and laterally to the boundaries of the ischemic lesions. In panel B, coronal slices highlight parahippocampal and hippocampal structures, including the fornix. The ischemic lesions lay inferiorly and posteriorly to the hippocampus and spare the fornix and the retrosplenial cingulate cortex.

1375x773mm (72 x 72 DPI)

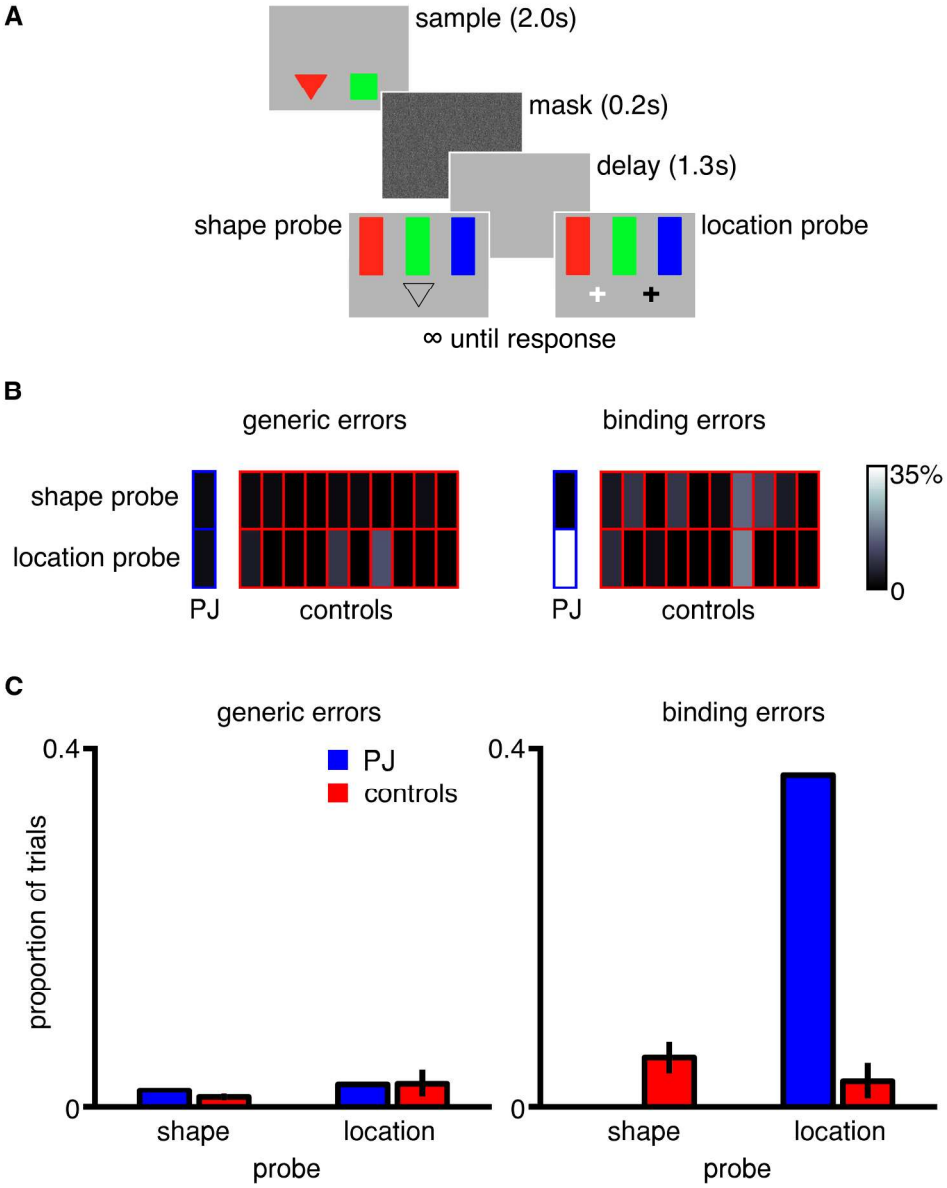

Figure 2. Spatial vs. non-spatial binding in working memory. Panel A shows the trial structure. The sample display for all participants (including PJ) contained a square and a triangle, placed side by side in the bottom half of the screen. The two objects were red, blue or green and never had the same colour. After a brief pattern mask and blank delay, three vertical coloured bars appeared as well as a cursor, which the participant used to report the colour of the memory target. In shape trials, targets were identified by a probe whose outline matched the target shape. In location trials, the location of targets were identified by a white cross. Panel B shows each individual participants' error rate on a greyscale, with lighter colours representing a higher proportion of errors; the left panel shows generic errors, the right panel shows binding errors. On each panel, the upper row shows errors following shape probes, while the lower row shows errors following location probes, for PJ (blue outline) and each of the controls (red outline). Panel C shows PJ's and the group averaged proportion of generic and binding errors. Error bars are standard error of the mean.

209x254mm (300 x 300 DPI)

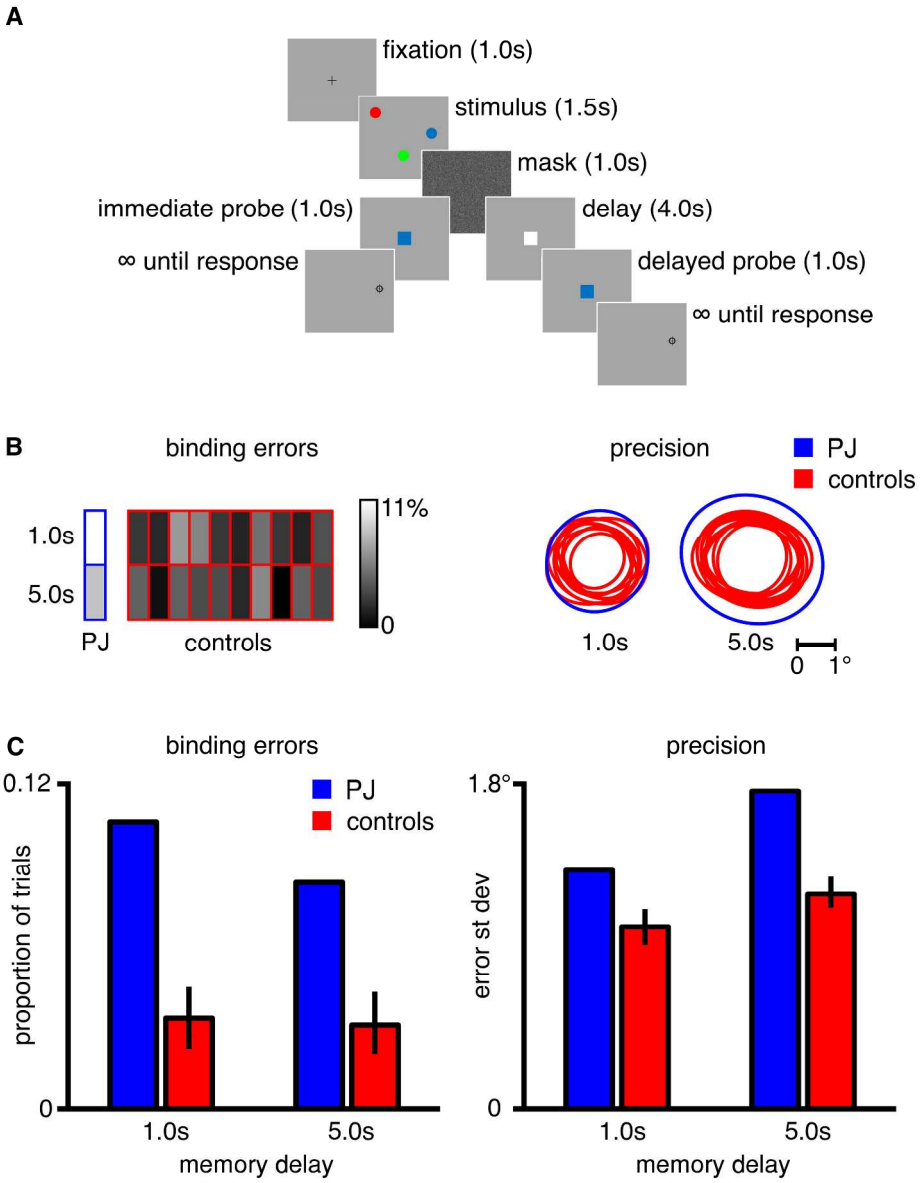

Figure 3. Delayed spatial recall. Panel A shows the structure of immediate and delayed, spatial recall trials. The sample display for all participants (including PJ) contained three coloured discs, which could appear in both the upper and lower portion of the screen. The participants had to reproduce the position of one of the discs (the target) using a mouse cursor after either a 1.0s pattern mask or an additional 4.0s delay. The target was identified by its colour, indicated by a visual probe displayed at the center of the screen. Panel B (left) shows PJ's (blue outline) and controls' (red outline) individual percentage of binding errors on a greyscale, following 1.0s (upper row) and 5.0s (lower row) delays, with lighter colours representing a higher proportion of errors. Panel B (right) shows recall precision (95% error ellipses) in 1.0s and 5.0s delayed recall trials for PJ (blue) and controls (red). Panel C shows PJ's and the group averaged proportion of binding errors and precision. Error bars are standard error of the mean.

209x270mm (300 x 300 DPI)

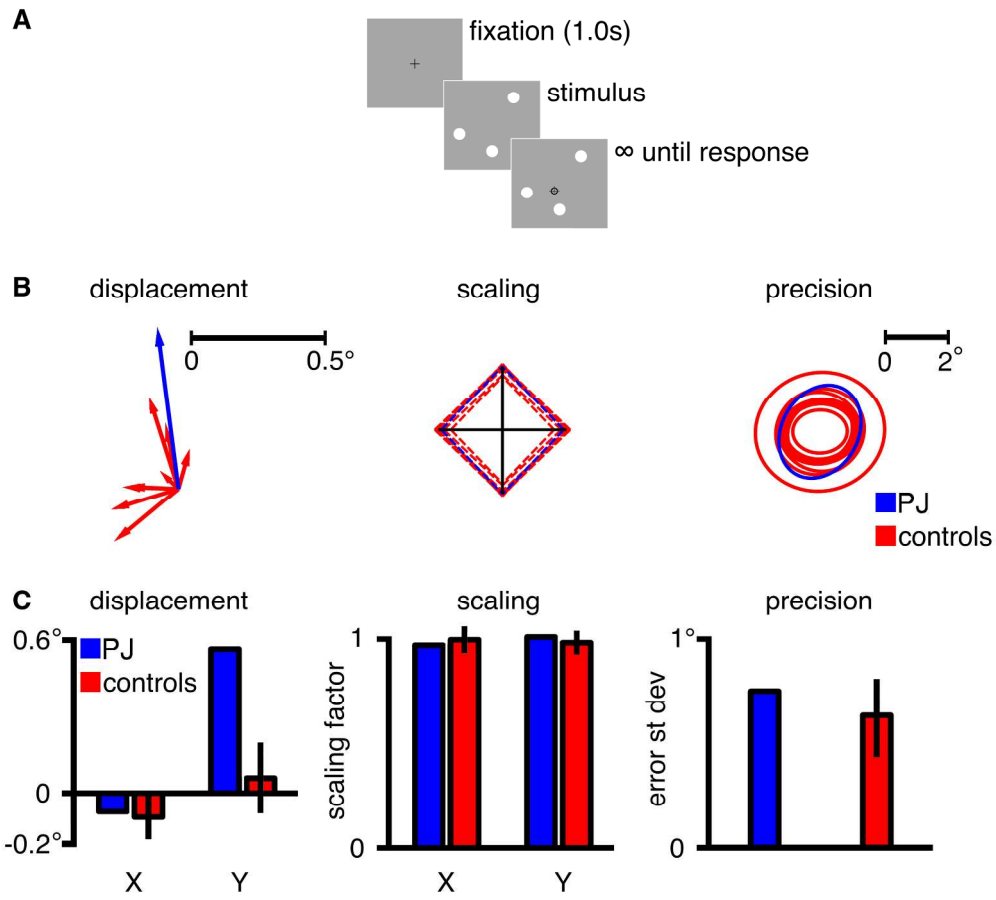

Figure 4. Centroid estimation. Panel A shows the trial structure. The participants placed a cursor at the centroid of the configuration formed by three bright discs. The discs remained visible until the participant made a response by clicking the mouse. Panel B shows each participant's constant displacement (arrow vectors), scaling (diamond plot) and precision (uncertainty ellipses) in locating the centroid. The length of the diamond plot's hemi-axes corresponds to 1.0 scaling factor. Panel C shows PJ's and group averaged values of the constant displacement and scaling factor, separately for azimuth (X) and elevation (Y). The precision measure shown is the square root of the mean error variance for azimuth and elevation. Error bars in all cases are standard error of the mean.

209x191mm (300 x 300 DPI)

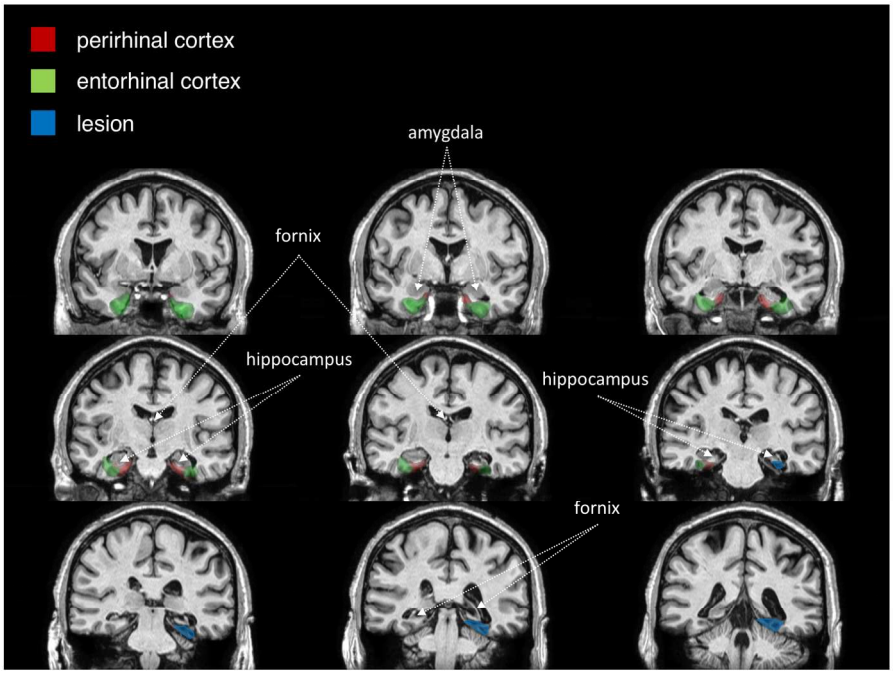

Figure S1. Multiple, MNI atlas registered coronal slices are displayed in neurological coordinates and show the relation between entorhinal and perirhinal cortex, and ischemic tissue, allowing a clearer depiction of the anatomical relation between these structures. The figure indicates that entorhinal and perirhinal cortex were spared by the ischemic event.

791x594mm (72 x 72 DPI)

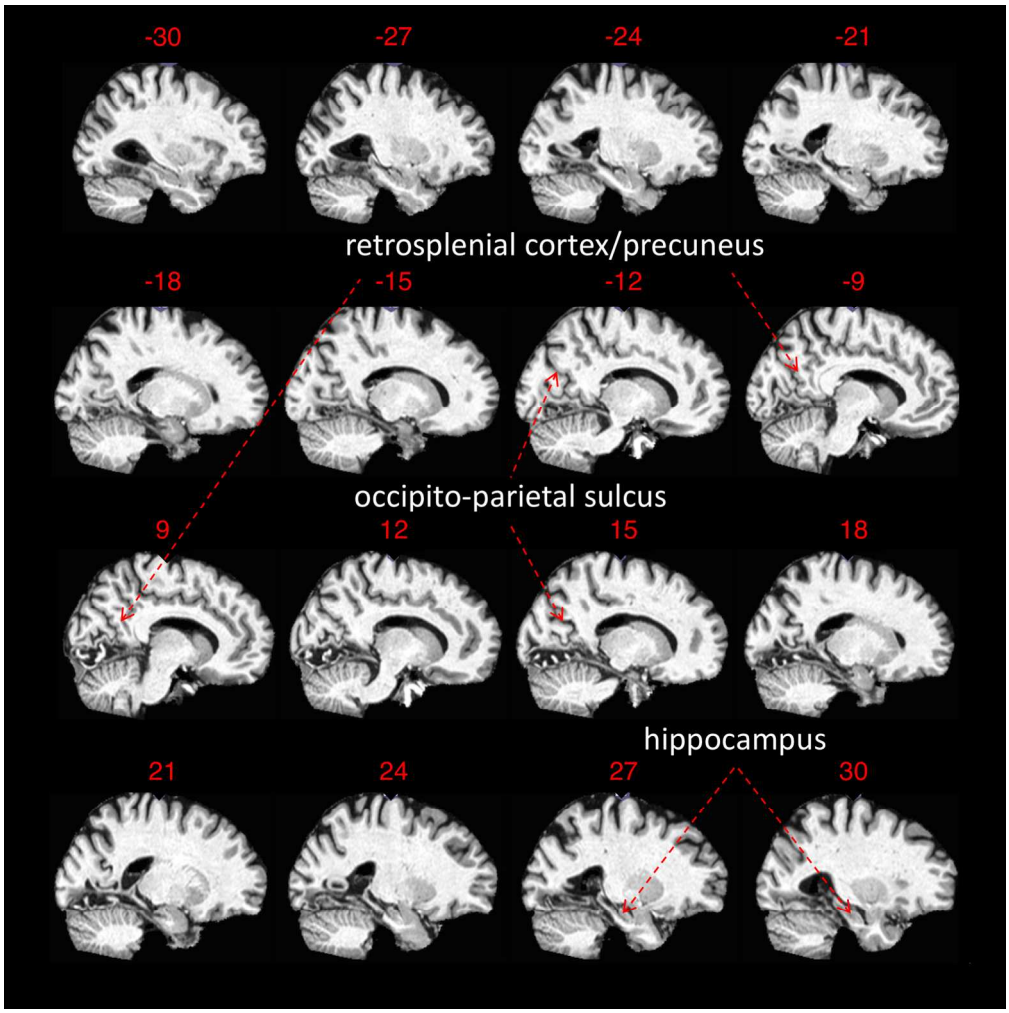

Figure S2. Multiple MNI atlas registered sagittal slices depict the relation between hippocampus and the lesioned parahippocampal and lingual cortex, in both hemispheres. Also, the restroplenial cingulate cortex and the precuneus are fully visible and show no evidence of ischemic damage.

791x793mm (72 x 72 DPI)

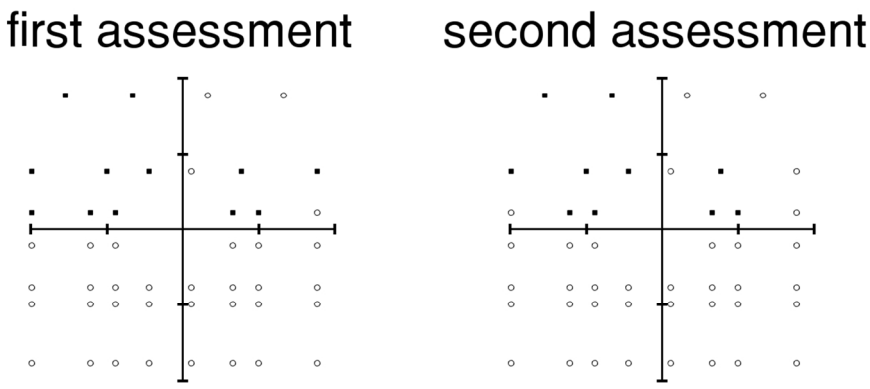

Figure S3. PJ's visual perimetry assessed three months (left panel) and five months (right panel) following the ischemic injury. Perimetry was measured with a binocular field test (Esterman, 1982). Hash marks on both the x and y axis indicate increments of ten visual degrees. Empty squares indicate hits, while filled squares indicate locations where PJ failed to report a target. PJ showed strict upper quadrantanopias, worse on the left than on the right. On the second assessment, PJ detected targets in the left and right upper visual field, at locations (-10.0°,2.29°) and (17.6°,7.90°), that he previously missed, suggesting partial recovery.

493x205mm (72 x 72 DPI)

Supplementary figure captions

Figure S1. Multiple, MNI atlas registered coronal slices are displayed in neurological coordinates and show the relation between entorhinal and perirhinal cortex, and ischemic tissue, allowing a clearer depiction of the anatomical relation between these structures. The figure indicates that entorhinal and perirhinal cortex were spared by the ischemic event.

Figure S2. Multiple MNI atlas registered sagittal slices depict the relation between hippocampus and the lesioned parahippocampal and lingual cortex, in both hemispheres. Also, the restroplenial cingulate cortex and the precuneus are fully visible and show no evidence of ischemic damage.

Figure S3. PJ's visual perimetry assessed three months (left panel) and five months (right panel) following the ischemic injury. Perimetry was measured with a binocular field test (Esterman, 1982). Hash marks on both the x and y axis indicate increments of ten visual degrees. Empty squares indicate hits, while filled squares indicate locations where PJ failed to report a target. PJ showed strict upper quadrantanopias, worse on the left than on the right. On the second assessment, PJ detected targets in the left and right upper visual field, at locations (-10.0°,2.29°) and (17.6°,7.90°), that he previously missed, suggesting partial recovery.